

A COMPREHENSIVE STUDY OF NEUTRON STAR RETENTION IN GLOBULAR CLUSTERS

ERIC PFAHL AND SAUL RAPPAPORT

Department of Physics, Massachusetts Institute of Technology, Cambridge, MA, 02139

AND

PHILIPP PODSIADLOWSKI

Nuclear and Astrophysics Laboratory, Oxford University, Oxford, OX1 3RH, England, UK

Submitted to ApJ

ABSTRACT

Observations of very high speeds among pulsars in the Galactic disk present a puzzle regarding neutron stars in globular clusters. The inferred characteristic speed of single pulsars in the Galaxy is $\sim 5 - 10$ times as large as the central escape speed from the most massive globular clusters. It is then reasonable to ask why any pulsars are seen in globular clusters, whereas, in fact, quite a large number have been detected and as many as ~ 1000 are thought to be present in some of the richest clusters. A cluster that initially contains 10^6 stars should be able to produce $\lesssim 5000$ NSs, simply based upon the mass function. Therefore, it would seem that at least $10 - 20\%$ of the NSs initially formed in a massive cluster must be retained until the current epoch.

The recently derived distributions in natal “kick” speeds based upon isolated pulsars in the Galaxy are incompatible with the numbers of pulsars seen in certain globular clusters, if the cluster pulsars had isolated progenitor stars. This *retention problem* is a long-standing mystery. It has been suggested that the retention problem may be solved if one assumes that a large fraction of NSs in clusters were formed in binary systems. We present a thorough investigation of this possibility that involves a population study of the formation and evolution of massive binary systems.

We use a Monte Carlo approach to generate an ensemble of massive primordial binaries. Binary component masses and orbital parameters are chosen at random from appropriate distribution functions. Mass transfer begins when the more massive star evolves to fill its critical potential surface (Roche lobe). The mass transfer may be stable or dynamically unstable, depending on the structure of the mass donor and the mass ratio of the components. Dynamically unstable mass transfer leads to a common-envelope phase and a dramatic reduction in the orbital separation, while a modest change in separation is expected if the transfer is stable. In either case, the orbital evolution is followed with an analytic prescription. It is assumed that the entire hydrogen-rich envelope of the initially more massive star is removed in the mass transfer episode, exposing the star’s helium core. The eventual collapse and supernova explosion of the core is accompanied by sudden mass loss and an impulsive kick to the newly-formed neutron star.

If we apply the large mean neutron star kick speeds inferred from pulsar observations, we find that most binaries are unbound following the supernova, and all but a very small fraction of the liberated neutron stars are ejected from the cluster. As expected, the majority of retained NSs have massive companions. These massive retained binaries are mostly the product of stable mass transfer, where the initially less massive star accretes a significant fraction of the envelope of the neutron star progenitor. Systems that undergo dynamically unstable mass transfer shrink dramatically and acquire large relative orbital speeds (typically $\gtrsim 200 \text{ km s}^{-1}$). Sudden mass loss in the subsequent supernova explosion transforms $\gtrsim 10\%$ of the orbital speed into translational motion. If, in addition, the newly-formed neutron star receives a large kick, it is likely that the system will escape from the cluster.

Our “standard model” involving the formation of neutron stars in binary systems predicts that $\sim 5\%$ of the neutron stars initially formed in a massive cluster can be retained. Over a wide range of model parameters, the retention fraction varies from $\sim 1 - 8\%$. When a number of other effects are taken into account, e.g., a reasonable binary fraction among massive stars, the retention fraction becomes several times smaller. Therefore, we suggest that perhaps the conventional thinking regarding neutron star kicks must be modified or that a new paradigm must be adopted for the evolution of some of the most massive globular clusters in the Galaxy.

Subject headings: globular clusters: general — stars: neutron

1. INTRODUCTION

A growing body of observational and theoretical evidence suggests that some massive globular clusters may

contain more than ~ 1000 neutron stars (NSs). However, the presence of even as few as ~ 100 NSs is difficult to reconcile with the large NS “kicks” inferred from proper motion studies of single, young radio pulsars in the Galac-

tic disk. The problem is that globular clusters have central escape speeds $\lesssim 50 \text{ km s}^{-1}$, while it is widely thought that most NSs are born with speeds $\gtrsim 200 \text{ km s}^{-1}$. This is the essence of the NS *retention problem* in globular clusters.

If one accepts the conventional wisdom regarding NS kicks, then only a very small fraction of NSs that are remnants of isolated progenitors should be retained in a globular cluster. Hansen & Phinney (1997) found that a Maxwellian distribution in kick speeds, with a mean of $\sim 300 \text{ km s}^{-1}$, is consistent with data on pulsar proper motions. This distribution predicts that only $\sim 0.4\%$ of NSs are born with speeds $< 50 \text{ km s}^{-1}$, and $\sim 3\%$ with speeds $< 100 \text{ km s}^{-1}$. If one adopts an initial mass function derived from stars in the solar neighborhood (e.g., Kroupa, Tout, & Gilmore 1993), it can be shown that $\lesssim 5000$ NSs will be formed in a cluster that initially contains 10^6 stars. A retention probability of 1% predicts that $\lesssim 50$ NSs should be present in a massive globular cluster such as 47 Tuc, where we have assumed that the cluster has not lost a significant fraction of its mass. Such a small number of NSs in 47 Tuc is incompatible with the observational sample of more than 20 millisecond radio pulsars (Camilo et al. 2000) when selection effects are taken into account.

Drukier (1996; using the results of Brandt & Podsiadlowski 1995) and Davies & Hansen (1998) have demonstrated quantitatively that if a NS is formed in a massive binary system, then there is a significant probability that the NS will remain in the binary following the supernova (SN) explosion, and that the recoil speed of the system could be sufficiently small to allow it to be retained in the cluster. While these studies provided a useful verification of the potential importance of massive binaries, they did not involve a systematic population study to determine a realistic NS retention fraction.

Our primary goal in this paper is to make a detailed quantitative assessment of the role of massive binaries in retaining NSs in globular clusters. This calls for a realistic description of the population of primordial binaries, as well as a sufficiently detailed consideration of the relevant stellar evolution processes that precede the first SN explosion. To this end, we have developed a Monte Carlo population synthesis code that follows each of an ensemble of massive, primordial binaries from the main-sequence phase, through any important episodes of mass transfer, up to and immediately beyond the time of the first SN.

We have attempted to make the paper self-contained, so that much of the relevant background material and associated references are provided. The paper is organized as follows. In § 2 we review the evidence indicating that NSs may be quite abundant in certain massive globular clusters. An historical overview of the debate regarding NS kicks is presented in § 3. In § 4 we describe the various elements of our Monte Carlo population synthesis code. A semi-analytic treatment of massive binary population synthesis and NS retention is given in § 5, which we intend to facilitate the interpretation of the results of our detailed numerical calculations presented in § 6. The main results of our study are reviewed in § 7, and we evaluate the possibility that binaries provide a robust solution to the retention problem. Finally, we speculate in § 8 on possible alternative solutions to the NS retention problem.

2. NEUTRON STARS IN GLOBULAR CLUSTERS

Several tens of millisecond pulsars (MSPs), a dozen bright X-ray sources, and numerous low-luminosity X-ray sources have been detected in the Galactic globular cluster system. See Table 1 for a list of clusters that may contain large numbers of NSs. The nature of the pulsars is clear: these are rapidly spinning NSs, many of which have binary companions. The luminous cluster X-ray sources are all low-mass X-ray binaries (LMXBs) powered by accretion onto a NS. An accepted familial relationship exists between LMXBs and the majority of MSPs, the former being the evolutionary progenitors of the latter. Recent observations (Grindlay et al. 2001) provide tantalizing evidence that many of the low-luminosity X-ray sources may be MSPs for which radio pulsations have not yet been detected (see, however, Pfahl & Rappaport 2001).

More refined pulsar searches, deeper X-ray observations, and thorough theoretical population studies will advance our understanding of the cluster population of NSs, and in turn may provide powerful new insights into the formation and evolution of globular clusters. We now briefly review what is known and what is speculated regarding NSs in globular clusters.

2.1. Millisecond Pulsars

Camilo et al. (2000; see also Freire et al. 2000), using the Parkes radio telescope, have detected more than 10 MSPs in the globular cluster 47 Tuc, bringing the current total to over 20. With a cursory analysis of the selection effects and a reasonable pulsar luminosity function, Camilo et al. (2000) estimated that 47 Tuc may contain ~ 200 potentially observable MSPs, and therefore the total number of NSs in 47 Tuc is expected to be even larger.

47 Tuc is a rich and relatively nearby cluster (distance $\sim 4.5 \text{ kpc}$), and thus has been the subject of much study, especially in recent years. Unfortunately, other clusters with properties similar to 47 Tuc have not yet received as much attention. However, there is compelling observational evidence that at least one other cluster contains in excess of 100 NSs. Fruchter & Goss (2000) found significant diffuse radio emission from the core of the massive globular cluster Terzan 5. These authors estimated that this diffuse component may be attributable to between 60 and 200 potentially observable pulsars, and claim that this range may represent a rather severe underestimate of the total number of pulsars in the cluster. Thus far, two MSPs have been detected in Terzan 5 (Lyne, Mankelov, Bell, & Manchester 2000).

2.2. X-ray Sources

Many of the members of the well-known class of bright X-ray sources in globular clusters, with X-ray luminosities $L_X \sim 10^{36} - 10^{38} \text{ ergs s}^{-1}$ (see Deutsch, Margon, & Anderson 2000, and references therein), exhibit type I X-ray bursts (Lewin, van Paradijs, & Taam 1993) and are therefore accreting NSs in binary systems. In fact, 7 of the 12 known bright sources have a well-measured or constrained binary period (Deutsch, Margon, & Anderson 2000). Each of these objects resides in a different globular cluster (Table 1). While this sample of X-ray binaries does not constitute a large number of NSs in itself, the existence and

TABLE 1
NEUTRON STARS IN GLOBULAR CLUSTERS

Cluster	Luminous ^a X-ray Sources	Low-luminosity ^b X-ray Sources	Radio Pulsars	Distance ^c (kpc)	[Fe/H] ^c	$\log \rho_0^c$ ($M_\odot \text{ pc}^{-3}$)
Liller 1	1	0	0	10.5	0.22	5.9
NGC 104/47 Tuc	0	108 ^d	>20 ^e	4.5	-0.76	5.3
NGC 1851	1	0	0	12.1	-1.22	5.8
NGC 5904/M5	0	9	2 ^f	7.5	-1.29	4.4
NGC 6205/M13	0	12	2 ^g	7.7	-1.54	3.8
NGC 6397	0	14	1 ^h	2.3	-1.95	6.2
NGC 6440	1	0	1 ⁱ	8.4	-0.34	5.8
NGC 6441	1	0	0	11.2	-0.53	5.7
NGC 6624	1	0	2 ^j	8.0	-0.42	5.7
NGC 6652	1	0	0	9.6	-0.96	5.0
NGC 6712	1	0	0	6.9	-1.01	3.6
NGC 6752	0	13	5 ^h	4.0	-1.56	5.4
NGC 7078/M15	1	0	8 ^g	10.3	-2.25	5.9
Terzan 1	1	0	0	6.2	-0.35	4.0
Terzan 2	1	0	0	8.7	-0.40	5.1
Terzan 5	1	0	2 ^k	7.6	-0.28	5.9
Terzan 6	1	0	0	9.5	-0.50	5.9

References. — (a) Deutsch, Margon, & Anderson 2000; (b) Verbunt 2001, unless otherwise noted; (c) Harris 1996; (d) Grindlay et al. 2001; (e) Camilo et al. 2000; (f) Anderson et al. 1997; (g) Anderson 1993; (h) D’Amico et al. 2001; (i) Lyne, Manchester, & D’Amico 2001; (j) Biggs et al. 1994; (k) Lyne et al. 2000

properties of these systems may have important implications regarding the evolution of the NS population in their respective host clusters (see § 2.3 below).

Not as well known, and certainly not as well understood, is the class of low-luminosity cluster X-ray sources (e.g., Johnston & Verbunt 1996; Verbunt 2001), with $L_X \sim 10^{31} - 10^{34} \text{ ergs s}^{-1}$, where the lower limit is set by detection sensitivities. Prior to the launch of the *Chandra X-ray Observatory*, fewer than 50 of these faint sources had been discovered in the entire Galactic globular cluster system (see Verbunt 2001 for a recent analysis of the *ROSAT* database), primarily with the *ROSAT* and *Einstein* satellites. However, recent deep *Chandra* observations of 47 Tuc have revealed $\gtrsim 100$ faint sources in this cluster alone (Grindlay et al. 2001), whereas only 9 had been confirmed previously (Verbunt & Hasinger 1998). There is growing evidence that the majority of the faint X-ray sources in 47 Tuc may be NSs, perhaps MSPs that have not yet been detected at radio wavelengths. All of the 15 MSPs in 47 Tuc with well-measured radio timing positions (Freire et al. 2000) have counterparts in the *Chandra* images (Grindlay et al. 2001). Further multiwavelength observations are required to determine the true distribution of objects contributing to the population of low-luminosity sources.

2.3. Theoretical Considerations

Variations in the number of detected radio pulsars and X-ray sources from cluster to cluster may be attributed to the distances of the clusters, selection effects inherent in the observations, as well as differences between the intrinsic NS populations. Predictions of the total number of potentially observable NSs – in the form of MSPs or accretion-powered X-ray sources – present in a globular cluster are difficult. Empirical likelihood estimates based on the observational sample are hindered by small-

number statistics and uncertainties regarding selection effects. Theoretical studies aimed at accounting for the numbers and properties of the detected pulsars involve models that utilize various uncertain stellar evolution and dynamical processes.

Large-scale population studies of the formation and evolution of X-ray binaries and MSPs in globular clusters have only recently been undertaken (see Davies 1995; Sigurdsson & Phinney 1995; Rasio, Pfahl, & Rappaport 2000; Rappaport et al. 2000). The dense stellar environment in a globular cluster allows for dynamical binary formation channels not possible in the Galactic disk, such as two-body tidal capture (e.g., Fabian, Pringle, & Rees 1975; Rasio & Shapiro 1991; DiStefano & Rappaport 1992), and three- and four-body exchange processes (e.g., Hills 1976; Hut, Murphy, & Verbunt 1991; Sigurdsson & Phinney 1993; Bacon, Sigurdsson, & Davies 1996; Rasio, Pfahl, & Rappaport 2000). The absolute probabilities of dynamical encounters depend on the local stellar environment and thus implicitly on the dynamical evolution of the cluster. This nonlinear linkage between *local* dynamical processes and the *global* cluster evolution poses significant computational problems, but the potential rewards are far-reaching. Such population studies promise to be a powerful tool that relates the current NS population to the formation and evolution of globular clusters.

Preliminary calculations (Rasio, Pfahl, & Rappaport 2000; Rappaport et al. 2000) indicate that a large initial pool of single NSs ($\sim 10^4$) may be required to explain the handful of very short-period binary radio pulsars in 47 Tuc; i.e., the formation efficiency is quite low. Short-period binary MSPs and LMXBs in other clusters may be good indicators of an initially large number of NSs in those clusters as well. The purpose of the present paper is to investigate the conditions that favor the retention of such a large NS population.

3. NEUTRON STAR KICKS

It was suggested four decades ago by Blaauw (1961; see also Boersma 1961), before the discovery of the first radio pulsar (Hewish et al. 1968), that there may be a population of massive-star remnants (neutron stars) in the Galaxy with anomalously large space velocities, acquired when the NS progenitor explodes in a binary system. If the orbit is circular and the explosion is spherically symmetric, then the compact remnant is liberated from its companion if more than one-half of the initial mass of the binary is lost in the SN. Blaauw (1961) proposed this mechanism to explain the famous “runaway” O and B stars (see Hoogerwerf, de Bruijne, & de Zeeuw 2001 for a recent discussion).

Gunn & Ostriker (1970) analyzed the data on some forty pulsars known at that time. They found that the pulsars had an average scale height of ~ 120 pc above the Galactic plane, in contrast to the smaller scale height (~ 50 pc) of massive O and B stars. Gunn & Ostriker (1970) concluded that pulsars are born with an average speed of ~ 100 km s $^{-1}$, and attributed this speed to a binary origin.

By 1980, 26 pulsars had reasonably accurate interferometrically determined proper motions. Lyne, Anderson, & Salter (1982) showed that the observed pulsars had a three-dimensional rms speed of ~ 210 km s $^{-1}$, and a vertical scale height of ~ 350 pc. Thus, pulsars are even faster and more dispersed than indicated in the study by Gunn & Ostriker (1970). Based on the data of Lyne, Anderson, & Salter (1982), Paczyński (1990) adopted a modified Lorentzian distribution of pulsar speeds,

$$p(v_k) = \frac{4}{\pi} \frac{1}{v_0} \left[1 + \left(\frac{v_k}{v_0} \right)^2 \right]^{-2}, \quad (1)$$

where v_0 is the rms speed. The best agreement with the data was found with $v_0 = 270$ km s $^{-1}$.

The next major step in the study of the kinematics of the Galactic pulsar population came with the work of Lyne & Lorimer (1994). This analysis considered a total of 99 pulsars, 86 of which had interferometric proper motions or upper limits, and an additional 13 pulsars with only scintillation speed measurements (e.g., Cordes 1986). Helfand & Tademaru (1977) and Cordes (1986) noted a strong selection effect against detecting high-velocity pulsars. Fast pulsars born in the Galactic disk rapidly move away from the plane and may only spend a small fraction of their radio lifetimes in the flux-limited volume. The vertical egress of fast pulsars thus implies a mean speed for the detectable pulsar population that is lower than the true mean pulsar birth speed. Lyne & Lorimer (1994) attempted to account for this effect by utilizing only those pulsars with characteristic ages less than 3 Myr, thus reducing the analyzed sample to 29 objects. Using a revised dispersion-measure distance scale (Taylor & Cordes 1993), Lyne & Lorimer (1994) derived a mean pulsar speed of ~ 450 km s $^{-1}$ and indicated that $\lesssim 1\%$ of pulsars have speeds less than 50 km s $^{-1}$.

The larger proportion of fast pulsars (speeds $\gtrsim 200$ km s $^{-1}$) began to cast doubt on the notion that the high velocities were acquired as a result of the binary “slingshot” effect (see, however, Iben & Tutukov 1996 and the rebuttal by van den Heuvel & van Paradijs 1997). Shklovskii (1970)

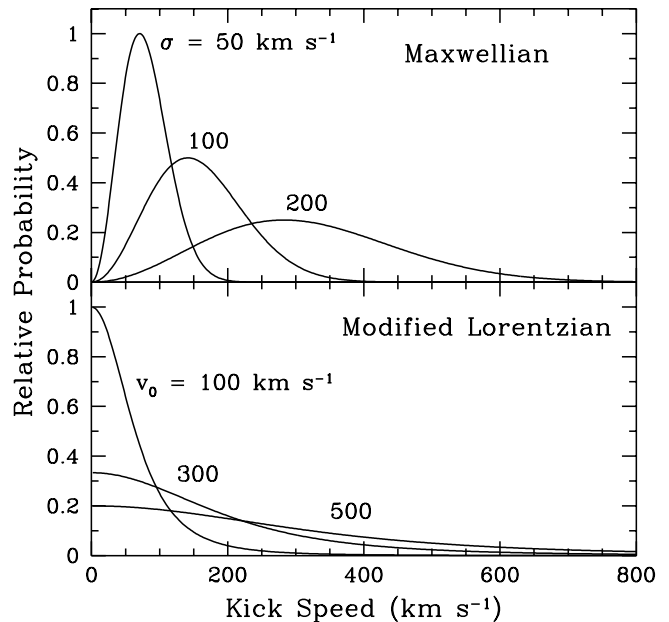


FIG. 1.— The Maxwellian and modified Lorentzian kick distributions, shown for σ (km s $^{-1}$) = {50, 100, 200} and v_0 (km s $^{-1}$) = {100, 300, 500}, respectively.

was the first to suggest that large pulsar speeds may result from an asymmetry intrinsic to the SN explosion. This is now a widely held view. Proposed physical mechanisms for natal NS kicks include purely hydrodynamical models, as well as scenarios that involve asymmetric neutrino emission, possibly correlated with the orientation and strength of the magnetic field within the proto-neutron star (Arras & Lai 1999). For a recent review of various natal kick mechanisms, see Lai (2000). Harrison & Tademaru (1975; see also Lai, Chernoff, & Cordes 2001) have proposed an alternative mechanism for the acceleration of pulsars that involves asymmetric dipole radiation *after* the pulsars has been formed, the so-called “electromagnetic rocket” mechanism.

Since the work of Lyne & Lorimer (1994), a number of authors have reanalyzed the pulsar proper motion data with more sophisticated treatments of selection effects (e.g., Lorimer, Bailes, & Harrison 1997; Hansen & Phinney 1997; Cordes & Chernoff 1998). Each of these studies employed a different statistical methodology, but all found a mean three-dimensional pulsar speed in excess of 300 km s $^{-1}$. Lorimer, Bailes, & Harrison (1997) and Hansen & Phinney (1997) found that a Maxwellian distribution in natal kick speeds, of the form

$$p(v_k) = \sqrt{\frac{2}{\pi}} \frac{v_k^2}{\sigma^3} e^{-v_k^2/2\sigma^2}, \quad (2)$$

was reasonably consistent with the proper motion data, with $\sigma \sim 300$ km s $^{-1}$ and ~ 200 km s $^{-1}$, respectively, in the two studies. Cordes & Chernoff (1998) found evidence for a bimodal kick distribution, with $\gtrsim 86\%$ of the pulsars contained in a Maxwellian component with a dispersion of $\sigma \lesssim 200$ km s $^{-1}$, and the remaining NSs contained in a high-speed component with a dispersion of ~ 700 km s $^{-1}$. In all of these investigations, a Maxwellian distribution was adopted by convention. However, both Lorimer, Bailes, & Harrison (1997) and Hansen & Phinney (1997) stress that, while it is likely that the mean birth

speed of pulsars is large, and that high-velocity pulsars are under-represented in the observational sample, the data do not constrain the functional form of the underlying kick distribution (see also, Fryer, Burrows, & Benz 1998), nor do the data suggest a physical mechanism for the kick.

For completeness, we also list a number of pieces of indirect evidence for NS kicks.

(1) Pulsar velocities $\gtrsim 1000 \text{ km s}^{-1}$ have been inferred from pulsar-supernova remnant associations (e.g., Caraveo 1993; Frail, Goss, & Whiteoak 1994) by dividing the distance from the rough geometrical center of the remnant by the characteristic spin-down age of the pulsar; however, the reliability of some of these estimates is questionable (see Gaensler & Frail 2000).

(2) For two compact double neutron star systems not in a globular cluster, PSR 1913+16 and PSR 1534+12, Fryer & Kalogera (1997; see also Flannery & van den Heuvel 1975) estimate that the most recently formed NS in each case had a kick of $\gtrsim 200 \text{ km s}^{-1}$.

(3) Kaspi et al. (1996) have found that the B-star companion to the pulsar PSR J0045-7319 in the SMC has a spin that is inclined with respect to the orbital angular momentum vector, and may, in fact, have retrograde rotation. This is convincing evidence that the pulsar received a kick with a significant component perpendicular to the pre-SN orbital plane.

(4) Systems with moderate-to-high eccentricities ($e \gtrsim 0.3$) seem to dominate the sample of Be/X-ray binaries with measured orbital parameters (see Bildsten et al. 1997). These eccentricities may require kick speeds $\gtrsim 50 \text{ km s}^{-1}$ (Verbunt & van den Heuvel 1995). However, a number of Be/X-ray binaries (XTE J1543-568, 4U 0352+30/X Per, 2S 1553-54, GS 0834-43, γ Cas; see Table 6) exhibit relatively low eccentricities ($e \lesssim 0.2$) and orbital periods sufficiently long that tidal circularization could not have played a role (Delgado-Martí et al. 2001). A detailed study of X Per/4U 0352+30 (Delgado-Martí et al. 2001) revealed that the present orbit ($P_{\text{orb}} = 250 \text{ d}$, $e = 0.11$) is entirely consistent with the neutron star having been born with no kick. This may indicate that the underlying NS kick distribution is not simply related to the speed distribution of isolated pulsars (see § 8.2).

Large uncertainties regarding natal NS kicks imply that a comprehensive population study must incorporate a variety of kick distributions. In our simulations of the formation of NSs in globular clusters, we consider a single-component Maxwellian kick distribution as well as the modified Lorentzian proposed by Paczyński (1990) (see Figure 1).

4. POPULATION SYNTHESIS OF MASSIVE BINARIES

Aside from what little information can be inferred from the current cluster population of stars, there is insufficient data to tightly constrain the distributions in main-sequence masses and orbital parameters of the massive primordial binaries in globular clusters. However, a combination of theoretical and empirical evidence suggests that the process of star formation (single and binary) is quite generic in a qualitative sense (e.g., Elmegreen 2000, and references therein), and that the general “rules” that apply to star formation in the Galactic disk may also apply to regions of high stellar density, such as globular clus-

ters. Fortunately, there is a large body of work on the binary population in the Galactic disk (e.g., Abt & Levy 1978; Kraicheva et al. 1978; Duquennoy & Mayor 1991). For these reasons, and for lack of any concrete alternative suggestions, our population synthesis study of massive binaries in globular clusters parallels similar studies of massive binaries in the disk (e.g., Podsiadlowski, Joss, & Hsu 1992; Terman, Taam, & Savage 1998).

Our population synthesis code is comprised of three basic elements, corresponding to the three main evolutionary stages of a massive binary: (i) the masses and orbital parameters are chosen from appropriate distribution functions, (ii) analytic approximations are used to follow the binary stellar evolution through any important episodes of mass transfer, and (iii) the dynamical influence of the first SN explosion is computed. We now discuss each of these elements in detail.

4.1. Primordial Binaries

We define a *massive* primordial binary as a system where at least one component has a large enough main-sequence mass that it would yield a neutron star remnant if left to evolve in isolation. The main-sequence mass threshold for NS formation is $\sim 8 M_{\odot}$, with a weak dependence on metallicity (see § 5). Hereafter, we refer to the initially more massive component of the binary as the *primary* and the initially less massive component as the *secondary*. The main-sequence masses of the primary and secondary are denoted by M_1 and M_2 , respectively, and we define the main-sequence mass ratio as $q = M_2/M_1 < 1$.

Various authors (e.g., Kraicheva et al. 1978; Duquennoy & Mayor 1991) have found that the primary masses in close binaries are consistent with the initial mass function (IMF) of single stars. We draw primary masses from a single power-law IMF, which is appropriate for massive stars (see Miller & Scalo 1979; Scalo 1986; Kroupa, Tout, & Gilmore 1993):

$$p(M_1) = (x-1)(M_{1,\text{min}}^{-x+1} - M_{1,\text{max}}^{-x+1})^{-1} M_1^{-x}, \quad (3)$$

where $M_{1,\text{min}} \sim 8 M_{\odot}$. We choose values of x in the range 2–3, where $x = 2.35$ corresponds to a Salpeter IMF (Salpeter 1955). For our standard model (see § 6.2.1), we adopt $x = 2.5$. An isolated star with $M_1 > M_{1,\text{max}}$ is assumed to leave a black hole remnant rather than a NS. The precise value of $M_{1,\text{max}}$ is unknown, but is probably $\gtrsim 30 M_{\odot}$. Because the IMF sharply decreases with increasing mass, our results do not depend strongly on the value of $M_{1,\text{max}}$.

It is generally believed that the main-sequence masses of binary components are correlated (e.g., Abt & Levy 1978; Garmany, Conti, & Massey 1980; Eggleton, Fitchett, & Tout 1989). Observations of massive binaries suggest that equal masses may be favored (e.g., Abt & Levy 1978; Garmany, Conti, & Massey 1980), presumably as a result of the formation process. However, serious selection effects hamper the determination of the true mass ratio distribution, and other authors have found that low-mass companions to massive primaries appear to be more likely (e.g., Mason et al. 1998; Preibisch et al. 2000). For the distribution function, $p(q)$, we consider both increasing and decreasing functions of q , as encapsulated by the power-law form

$$p(q) = (1+y)q^y, \quad (4)$$

for $y > -1$. We take $y = 0.0$ for our standard model (see § 6.2.1).

It is often assumed in population studies of the sort we have undertaken that the orbits of primordial binaries are circular. However, since the process of binary formation is only poorly understood, there is no a priori justification for suggesting that massive, primordial binaries should have small eccentricities. The situation is less clear in globular clusters, where dynamical interactions may influence binary formation (e.g., Price & Podsiadlowski 1995; Bonnell, Bate, & Zinnecker 1998). However, it is expected that the binary will eventually circularize if the orbit is sufficiently compact that mass transfer will take place. From here on we only consider circular primordial binaries.

There exists at least one important caveat to the circularization assumption stated above. Eccentricities of ~ 0.5 are seen among the wide, interacting VV Cephei binaries, which consist of a massive red supergiant and an early-type B star (e.g., Cowley 1969; Cowley, Hutchings, & Popper 1977). The VV Cephei systems are the widest of the known massive, interacting binaries, with periods $\gtrsim 10$ yr, and their significant eccentricities may indicate that not enough time has elapsed for the system to circularize. The growth of the large red-supergiant envelope occurs over a relatively short timescale of $< 10^5$ yr, while the circularization timescale varies as $(a/R)^8$ (e.g., Hut 1981), where a is the binary semimajor axis and R is the radius of the supergiant. Therefore, the components of the observed VV Cephei binaries have experienced strong tidal interactions only very recently, in terms of the evolutionary history of the more massive star.

The binary separation, a , is chosen from a distribution that is uniform in the logarithm of a (Abt & Levy 1978; see, however, Duquennoy & Mayor 1991):

$$p(a) = \left[\ln \left(\frac{a_{\max}}{a_{\min}} \right) \right]^{-1} a^{-1} \quad (5)$$

For given component masses, the lower limit, a_{\min} , is determined from the constraint that neither star overflows its Roche lobe on the main sequence. The upper limit, a_{\max} , is somewhat arbitrary; in practice, we assume $a_{\max} = 10^3$ AU.

4.2. Mass Transfer: Overview

Owing to its larger mass, the primary will be the first star to leave the main sequence. The subsequent binary evolution depends on the size of the Roche lobe that surrounds the primary. For circular orbits, the volume-equivalent radius of the Roche lobe of the primary is well approximated by the formula due to Eggleton (1983):

$$\frac{R_{L1}}{a} \equiv r_{L1} = \frac{0.49}{0.6 + q^{2/3} \ln(1 + q^{-1/3})}, \quad (6)$$

where a in this equation represents the constant orbital separation. The radius of the Roche lobe of the secondary, R_{L2} , is obtained by replacing q in eq. (6) with $1/q$.

Left to evolve in isolation, the primary would grow to a maximum radius of $\sim 500 - 2000 R_{\odot}$ (the value depends sensitively on mass, metallicity, and especially assumptions about stellar winds). So, if the orbit is sufficiently compact ($R_{L1} \lesssim 20$ AU), the primary may grow to fill its Roche lobe. The value of ar_{L1} is used to determine

the evolutionary state of the primary when it begins to transfer matter through the inner Lagrange point.

It is particularly important to distinguish between mass transfer that is dynamically stable (proceeding on the nuclear or thermal timescale of the primary) and mass transfer that is dynamically unstable (proceeding on the dynamical timescale of the primary). For the case where the mass donor is more massive than the accretor, dynamical instability is typically attributed to one of two root causes. If the star grows faster than its Roche lobe (or the Roche lobe shrinks faster than the star does), a phase of runaway mass transfer may ensue. In particular, stars with deep convective envelopes tend to expand in response to mass loss (e.g., Paczyński & Sienkiewicz 1972; Hjellming & Webbink 1987), while the Roche lobe generally shrinks. Also, for systems with extreme mass ratios, the primary may not be able to achieve synchronous rotation with the orbit, causing the components to spiral together; this is the classic Darwin tidal instability (Darwin 1879; see also Hut 1981). The evolutionary state of the primary when it fills its Roche lobe is a good indicator of the physical character of the subsequent mass transfer and binary stellar evolution.

Following Kippenhahn & Weigert (1966; see also Lauterborn 1970 and Podsiadlowski, Joss, & Hsu 1992), we distinguish among three evolutionary phases of the primary at the onset of mass transfer. Case A evolution corresponds to core hydrogen-burning, Case B refers to the shell hydrogen-burning phase, but prior to central helium ignition, and case C evolution begins after helium is exhausted in the core. These three cases (see Figs. 2 and 3) provide a rough framework for categorizing binary stellar evolution during mass transfer. Of course, not all systems will undergo Roche lobe overflow. A large fraction of binaries will be sufficiently wide that the primary and secondary evolve as isolated stars prior to the first SN. We refer to such detached configurations as case D.

Of the three broad categories of mass transfer, case A evolution is potentially the most problematic. Perhaps the most likely outcome is a merger of the two stars following a contact phase, wherein both stars fill their Roche lobes, leaving a massive single star (Pols 1994; Wellstein, Langer, & Braun 2001). For a recent detailed discussion of the complex evolution processes that occur during case A mass transfer and the possible outcomes, see Nelson & Eggleton (2001) and Wellstein, Langer, & Braun (2001). Fortunately, the subtleties of case A evolution may essentially be overlooked in the present study. The range in orbital separations admitted by case A is $\sim 3 - 20 R_{\odot}$, which comprises $\sim 5 - 10\%$ of the primordial binary population. In addition, if the majority of case A systems merge as expected, then a detailed consideration of case A evolution is unnecessary, since our focus is on how binarity impacts the retention problem. In our population synthesis code, case A mass transfer is treated in precisely the same way as early case B mass transfer (see below). This treatment is certainly unrealistic, but it is a highly optimistic scenario in regard to the retention problem, and so functions to provide the maximum retention fraction for the case A systems.

Two important subcases comprise case B. *Early* case B (case B_e) mass transfer occurs when the primary fills

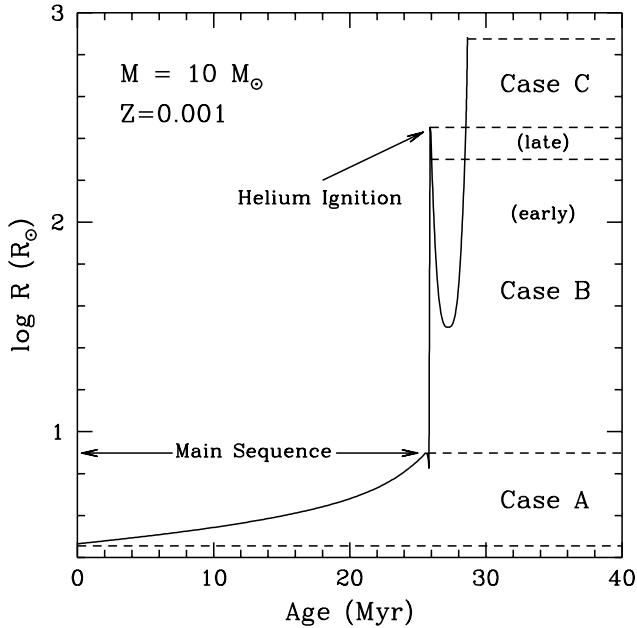


FIG. 2.— Evolution of the radius as a function of time for a star of mass $10 M_{\odot}$ and metallicity $Z = 0.001$. The range of radii for each case of mass transfer is labeled. Note that the radius decreases by a factor of ~ 10 immediately following central helium-ignition.

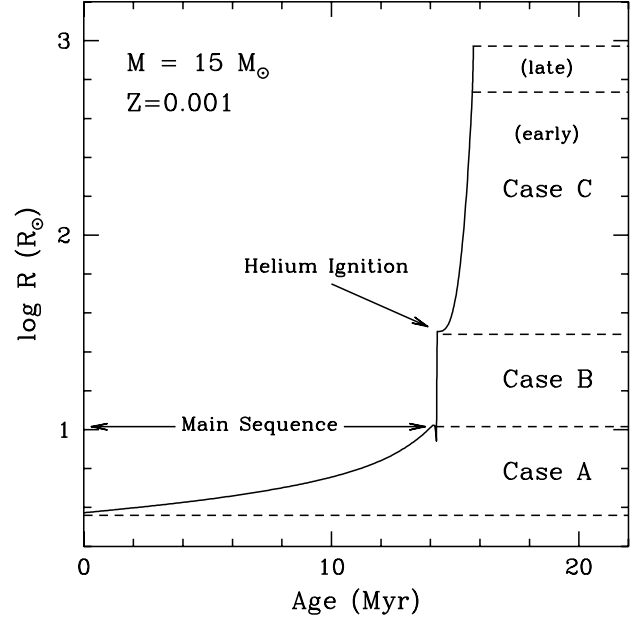


FIG. 3.— Evolution of the radius as a function of time for a star of mass $15 M_{\odot}$ and metallicity $Z = 0.001$. Helium ignites in the core while that star is evolving through the Hertzsprung Gap. Steady helium-burning proceeds rapidly, and the radial evolution is barely perturbed during this phase, hence the term “failed blue loop.” This type of evolution permits *early*, or radiative, case C mass transfer.

its Roche lobe as it evolves through the Hertzsprung Gap (subgiant branch). In this case, the envelope of the primary is still mostly radiative and the mass transfer is thought to be initially stable for a wide range of mass ratios. *Late* case B (case B_l) mass transfer occurs when the primary fills its Roche lobe as it evolves up the first giant branch. Case B_l mass transfer is characterized by a deep convective envelope, in which case it is likely that mass transfer will initially take place on the dynamical timescale of the primary, leading to a common-envelope (CE) phase (see § 4.3). The range in orbital separations of case B systems is $\sim 20 - 1000 R_{\odot}$, which contains 30–40% of the primordial binary population.

For stars of mass $\lesssim 12 - 15 M_{\odot}$, core helium-burning is typically accompanied by a significant decrease in stellar radius (see Fig. 2), so that the primary cannot fill its Roche lobe during this time. After helium is exhausted in the core, the star develops a deep convective envelope and begins to ascend the Hayashi track. We refer to this phase as late case C (case C_l). We assume that case C_l mass transfer is dynamically unstable, as we do for case B_l (see, however, Podsiadlowski, Joss, & Hsu 1992; Podsiadlowski et al. 1994).

For stars more massive than $\sim 12 - 15 M_{\odot}$, stellar evolution calculations do not provide a self-consistent physical picture that simultaneously accounts for observations of massive stars in high- and low-metallicity environments (e.g., the Milky Way and the SMC, respectively). One main problem is to explain the ratio of blue to red supergiants among massive stars, as a function of metallicity (see Langer & Maeder 1995). For these massive stars, it is possible for helium to ignite in the core while the star

is traversing the Hertzsprung gap and is still mostly radiative. It is unclear how the radius behaves during the subsequent phase of core helium-burning. The radius may shrink somewhat, so that Roche lobe overflow is impossible during this phase. However, the radius may continue to increase after a short plateau (a so-called “failed blue loop” in the HR diagram; see Fig. 3). Therefore, it is theoretically possible for mass transfer to begin during core helium-burning, but the allowed range in stellar radii is sufficiently small that we neglect this possibility. Following core helium-exhaustion, the star still has a radiative envelope. Early case C (case C_e) mass transfer is possible before the primary reaches the base of the asymptotic giant branch and begins to ascend the Hayashi track, at which point the star is mostly convective and falls into the case C_l category. Cases C_e and C_l account for $\sim 15\%$ and $\sim 10\%$ of the primordial binaries, respectively.

Depending on the choice of a_{\max} , the fraction of binaries that remain detached prior to the first SN (case D) is between 30% and 60%. For solar metallicity, stars of mass $\gtrsim 20 - 25 M_{\odot}$ may shed their hydrogen-rich envelopes following core helium-exhaustion as a result of prodigious wind mass loss (Maeder 1992). However, for low-metallicity environments like globular clusters ($Z \lesssim 0.001$ typically), stellar wind mass loss is probably only important above $\sim 30 - 40 M_{\odot}$ (Maeder 1992), although it should be emphasized that such mass loss is quite uncertain, both theoretically and observationally. In our simulations, we assume that no mass is lost prior to the SN explosion. Clearly, since case D binaries are weakly bound, they make a negligible contribution to the NS retention fraction when the kick speeds are large.

The mass of the primary and its radius at the onset of Roche lobe overflow are sufficient to determine the category of mass transfer. Using the fitting formulae of Hurley, Pols, & Tout (2000), we compute the radius of an isolated star with the mass of the primary at different stages of its evolution (e.g., main sequence, core helium-ignition, base of the asymptotic giant branch). The Roche lobe radius of the primary falls into some range and determines if mass transfer is categorized as case A, B_e, B_l, C_e, C_l, or D.

It is worth adding a note here regarding the possible outcomes of contact evolution. Unless the initial mass ratio is close to unity, it is likely that the majority of case A, B_e, and C_e systems will evolve into a contact configuration (Pols 1994; Nelson & Eggleton 2001; Wellstein, Langer, & Braun 2001). Shortly after the primary first fills its Roche lobe, the mass transfer rate rises to values of order $M_1/\tau_{\text{th},1} \sim 10^{-3} - 10^{-4} M_\odot \text{ yr}^{-1}$, where $\tau_{\text{th},1}$ is the thermal timescale of the primary. Most of the envelope of the primary is removed during this initial rapid phase. The secondary reacts to donated material on its own thermal timescale, and thus can only accrete in an equilibrium fashion if it is very nearly coeval with the primary at the onset of Roche lobe overflow (i.e., $q \sim 1$). If the secondary is essentially unevolved at the time the primary fills its Roche lobe, the transferred gas will fill up the Roche lobe of the secondary and thus initiate a contact phase.

Some attempts have been made to follow the evolution of both stars during the contact phase (see Kähler 1989 for an overview of some of the important issues), but since the problem requires certain three-dimensional hydrodynamical elements, no complete physical description of this process has emerged. However, there are two distinct possible outcomes: (i) evolution during contact is dynamically stable, with some fraction of the material ejected from the system, or (ii) there is sufficient drag on the secondary – owing to the extended common stellar envelope surrounding the system – that the binary components spiral together on a dynamical timescale, possibly resulting in the ejection of the common envelope or a merger of the two stars. Dynamical spiral-in cannot be the generic consequence of contact evolution, since then we would have great difficulty in explaining the observed long-period high-mass X-ray binaries in the Galaxy (see § 8.2).

We expect that there is some critical mass ratio, q_{crit} , that separates stable and dynamically unstable mass transfer. In our simulations, we typically choose $q_{\text{crit}} = 0.5$ for all case B_e and C_e systems, which implies that 50% of these binaries undergo dynamically unstable mass transfer for a flat distribution in initial mass ratios.

4.3. Mass Transfer: Analytic Prescriptions

Dynamically stable mass transfer can be reasonably well characterized by two dimensionless parameters, not necessarily fixed during the evolution. The secondary accretes a fraction β of the mass lost by the primary. Generally, β is a function of the component masses, the rate at which mass is transferred from the primary, and the evolutionary state of the secondary. The complementary mass fraction, $1 - \beta$, escapes the binary system, taking with it specific angular momentum α , in units of the orbital angular momentum per unit reduced mass, $(GM_b a)^{1/2}$, where $M_b = M_1 + M_2$

is the total binary mass.

For a circular orbit, the orbital angular momentum is given by

$$J = \frac{M_1 M_2}{M_b} (GM_b a)^{1/2}. \quad (7)$$

Logarithmic differentiation yields (e.g., Rappaport, Joss, & Webbink 1982)

$$\frac{\delta J}{J} = \frac{\delta M_1}{M_1} + \frac{\delta M_2}{M_2} - \frac{1}{2} \frac{\delta M_b}{M_b} + \frac{1}{2} \frac{\delta a}{a}, \quad (8)$$

where it is assumed that orbit remains circular during the evolution. From the definition of the capture fraction, β , it is clear that $\delta M_2 = -\beta \delta M_1$ and $\delta M_b = (1 - \beta) \delta M_1$. We neglect the coupling between the rotation of the Roche lobe-filling primary and the orbit. Therefore, variation in the orbital angular momentum is attributed solely to systemic mass loss, and it follows that

$$\delta J = \alpha (GM_b a)^{1/2} \delta M_b. \quad (9)$$

We consider one of two modes of angular momentum loss during stable mass transfer: mass that is lost from the system takes with it (1) a constant fraction of the specific orbital angular momentum (constant α), or (2) the specific angular momentum of the secondary. Constant values of α and β lead to one possible analytic solution of eq. (8) (Podsiadlowski, Joss, & Hsu 1992)

$$\left(\frac{a'}{a}\right)_1 = \frac{M'_b}{M_b} \left(\frac{M'_1}{M_1}\right)^{C_1} \left(\frac{M'_2}{M_2}\right)^{C_2}, \quad (10)$$

where

$$\begin{aligned} C_1 &\equiv 2\alpha(1 - \beta) - 2 \\ C_2 &\equiv -2\alpha\left(\frac{1}{\beta} - 1\right) - 2. \end{aligned} \quad (11)$$

Primes on the masses and semimajor axis indicate the values after some amount of mass has been transferred. This solution assumes $\beta > 0$. The solution for $\beta = 0$ (totally non-conservative mass transfer) is obtained by replacing $(M'_2/M_2)^{C_2}$ with $\exp[2\alpha(M'_1 - M_1)/M_2]$; clearly, M_2 remains fixed in this case. Figure 4 illustrates the evolution of $(a'/a)_1$ as a function of the fractional mass loss, $\Delta M_1/M_1 \equiv 1 - M'_1/M_1$, from the primary. For our standard model, we use eq. 10 to evolve the orbit, with $\alpha = 1.5$, a value characteristic of mass loss through the L2 point, and $\beta = 0.75$. These values imply that $(a'/a)_1 \sim 1$ for $\Delta M_1/M_1 \sim 0.8$.

A second analytic solution can be obtained for the case where β is constant and where matter lost from the system takes away the specific angular momentum of the accreting star (perhaps in the form of jets or an axisymmetric wind). In this scenario we have

$$\left(\frac{a'}{a}\right)_2 = \left(\frac{M'_b}{M_b}\right)^{-1} \left(\frac{M'_1}{M_1}\right)^{-2} \left(\frac{M'_2}{M_2}\right)^{-2/\beta}. \quad (12)$$

Note that the orbit always expands in this case. Furthermore, it can be shown that eq. (12) is a weak function of β , and so $(a'/a)_2$ closely follows the $\beta = 1$ solution for a wide range of initial mass ratios (within a factor of two).

Mass that is removed from the primary on a dynamical timescale cannot be assimilated by the secondary, which can only accept matter on its much longer thermal readjustment timescale. Consequently, the transferred material fills the Roche lobe of the secondary and a common-envelope (CE) phase is initiated (Paczynski & Sienkiewicz

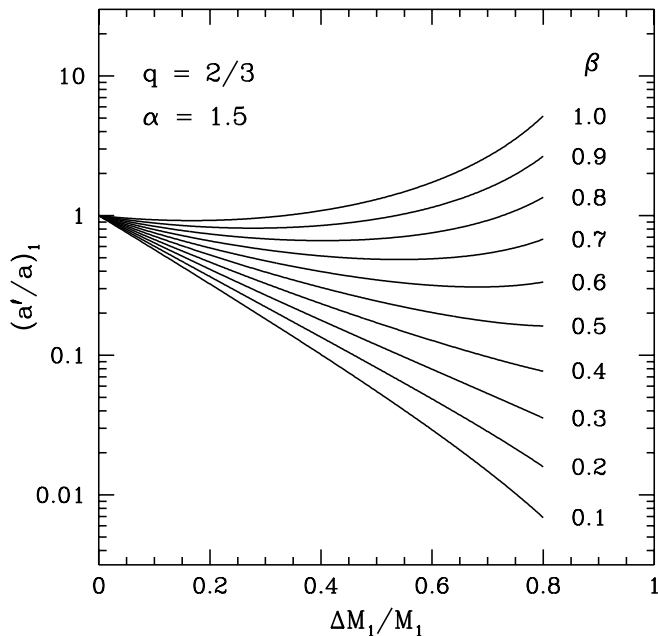


FIG. 4.— Curves representing the dependence of the final-to-initial orbital separation, $(a'/a)_1$, on the fractional mass loss from the primary, $\Delta M_1/M_1$, shown for ten different values of the mass capture fraction β . The initial mass ratio was chosen to be $q = 2/3$ and the dimensionless angular momentum-loss parameter was set to $\alpha = 1.5$, a value characteristic of mass loss through the L2 point.

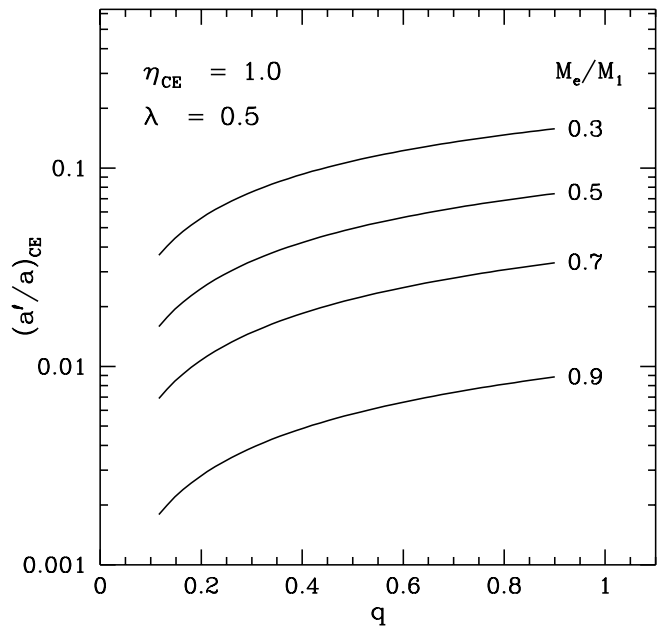


FIG. 5.— The final-to-initial orbital separation $(a'/a)_{\text{CE}}$ for common-envelope evolution as a function of the initial mass ratio, q . The function is plotted for four different values of the fractional envelope mass, M_e/M_1 , of the primary. For this plot, we have chosen $\eta_{\text{CE}} = 1.0$ and $\lambda = 0.5$.

1972). As a result of hydrodynamic drag, the secondary spirals in toward the core of the primary, depositing a fraction $\eta_{\text{CE}} \sim 1$ of the initial orbital binding energy into the CE as frictional luminosity (e.g., Meyer & Meyer-Hofmeister 1979; Sandquist, Taam, & Burkert 2000). For the binding energy of the envelope, we use the recent calculations of Dewi & Tauris (2000). If sufficient energy is available to unbind the envelope, what remains is a compact binary consisting of the secondary, which we assume is unaltered during the spiral-in process, and the helium-rich core of the primary. On the other hand, if the CE remains gravitationally bound to the system, drag forces will perpetuate the spiral-in and the two stars will merge.

A simple energy relation determines the outcome of the CE and spiral-in (e.g., Webbink 1984; Dewi & Tauris 2000):

$$-\frac{GM_1 M_e}{\lambda a r_{\text{L1}}} = \eta_{\text{CE}} \left[-\frac{GM_c M_2}{2a'} + \frac{GM_1 M_2}{2a} \right], \quad (13)$$

where M_e and M_c are the envelope-mass and the core-mass of the primary, respectively. The left-hand side of eq. (13) is the envelope binding energy, where λ is the structure constant computed by Dewi & Tauris (2000); for massive stars $\lambda \sim 0.5$. Solving eq. (13) for a'/a , we find

$$\left(\frac{a'}{a} \right)_{\text{CE}} = \frac{M_c M_2}{M_1} \left(M_2 + \frac{M_e}{2\eta_{\text{CE}} \lambda r_{\text{L1}}} \right)^{-1}. \quad (14)$$

If the secondary fills its Roche lobe for the computed final orbital separation, a' , this effectively indicates that insufficient energy was available to unbind the CE, and we assume that a merger is the result. Figure 5 illustrates the dependence of $(a'/a)_{\text{CE}}$ on the initial mass ratio, q , for four values of the initial fractional envelope mass, M_e/M_1 .

In all cases where a stellar merger is avoided, we assume that the entire hydrogen-rich envelope of the primary is removed, either transferred stably through the inner Lagrange point or expelled during a CE phase. By the time the primary reaches the base of the first giant branch (beginning of case B₁ evolution) its core is well developed, with a mass given approximately by (Hurley, Pols, & Tout 2000)

$$M_c \simeq 0.1 M_1^{1.35}. \quad (15)$$

We assume that this is the mass of the helium core immediately following case B_e mass transfer as well, although it is expected to be somewhat smaller, since mass transfer interrupts the evolution of the primary. For case C and D evolution, the mass of the core may be larger by $\sim 0.5 - 1 M_\odot$ as a result of shell nuclear-burning.

Following case B mass transfer, the exposed core of the primary is a nascent helium star. Helium stars with mass $\gtrsim 5 M_\odot$ probably experience mass loss in the form of a Wolf-Rayet wind, where the timescale for mass loss is comparable to the evolutionary timescale ($\sim 10^6$ yr) of the star (see Langer 1989). Stellar winds are less important for helium stars of lower mass. However, if $M_c \lesssim 3 M_\odot$ the star may grow to giant dimensions (Habets 1986b) upon central helium-exhaustion and possibly fill its Roche lobe, initiating a phase of case BB mass transfer (De Greve & de Loore 1977; Delgado & Thomas 1981; Habets 1986a). For the maximum radius of a helium star, we adopt a slightly modified version of the fitting formula derived by Kalogera

& Webbink (1998):

$$\log(R_{\text{He,max}}/R_{\odot}) = \begin{cases} 2.3 & M_c \leq 2.5 \\ 0.057[\log(M_c/M_{\odot}) - 0.17]^{-2.5} & M_c > 2.5 \end{cases} \quad (16)$$

This relation is consistent with the results of Habetz (1986b). It is expected that $\lesssim 1 M_{\odot}$ is transferred to the secondary during the case BB phase. As an example, suppose the secondary has a mass of $10 M_{\odot}$ following case B_e mass transfer, and the mass of the helium star is $3 M_{\odot}$, then the conservative transfer ($\beta = 1$) of $0.5 M_{\odot}$ from the helium star leads to a $\sim 30\%$ expansion of the orbit. We consider case BB mass transfer by assuming that a fixed amount of mass (e.g., $0.5 M_{\odot}$) is transferred conservatively to the secondary, and we expand the orbit accordingly. The inclusion of this process does not significantly influence our results.

4.4. Supernova Explosion

At the end of the mass transfer phase, the result may be a stellar merger or a binary consisting of the secondary and the core of the primary. Subsequently, the remaining nuclear fuel in the primary core is consumed, leading to core-collapse and a SN explosion. The post-SN orbital parameters are computed by taking into account the mass lost from the primary and the kick delivered to the newly-formed NS. In our simulations, we neglect the effect of the SN blast wave on the secondary. Statistically speaking, this assumption is well-justified, since only a small fraction of the binaries that we consider are sufficiently compact for the blast wave interaction to be important (e.g., Wheeler, Lecar, & McKee 1975; Fryxell & Arnett 1981; Livne, Tuchman, & Wheeler 1992; Marietta, Burrows, & Fryxell 2000).

The magnitude and direction of the kick to the NS are often assumed to be uncorrelated. There is, as yet, no clear observational indication that the directions of NS kicks are preferentially aligned with respect to the spin of the NS progenitor. We assume that the orientations of the kicks are distributed isotropically. If the directions of the kicks are confined to a small cone perpendicular to the pre-SN orbital plane, then the net retention fraction is actually likely to be smaller than in the isotropic case, when the characteristic kick speed is larger than the typical pre-SN binary orbital speed (see Appendix A).

One of two distinct outcomes follows the explosion: (i) the NS and the secondary are gravitationally bound, with new orbital parameters and a new CM velocity, or (ii) the binary is disrupted, with the NS and secondary receding along hyperbolic trajectories relative to the new CM. In the former case, the CM speed of the binary is compared to the cluster escape speed in order to determine if the NS, along with its binary companion, is retained in the cluster, while in the latter case the speed of the NS at infinity, computed in the pre-SN CM frame of reference, is compared to the escape speed.

When the characteristic kick speed is large, the mean eccentricity for the bound post-SN binaries may approach ~ 0.7 . In a significant fraction of these systems, the closest approach of the NS immediately after the SN is smaller than the radius of the secondary, with the likely outcome that the NS spirals in to the envelope of the secondary to

form a Thorne-Żytkow object (Leonard, Hills, & Dewey 1994; Brandt & Podsiadlowski 1995; see also § 6.5 for a more thorough discussion).

The computational procedure that we use to compute the dynamical influence of the SN explosion on the binary system is outlined in Appendix B. This approach allows for the possibility that the pre-SN binary is eccentric, and, for completeness, the mathematical formalism also includes the effects of the interaction between the secondary and the SN ejecta.

In the majority of our simulations, we apply a single escape speed to all of the stars and binaries in question. If this escape speed is identified with the depth of the potential well at the cluster center, then the computed retention fraction will be a maximum for a given set of parameters that describes the formation and evolution of the ensemble of binaries prior to the first SN. A more realistic cluster potential and spatial distribution of stars can only result in a smaller retention fraction. The flexibility of our population synthesis code makes it straightforward to assess how a more realistic model of the cluster effects our results (see § 6.4).

5. ANALYTIC ESTIMATES

In order to facilitate the interpretation of our detailed population synthesis calculations, it is useful to develop some quantitative insight regarding how different assumptions influence the NS retention fraction. This section is devoted to a semi-analytic population study of massive binaries and NS formation. We highlight the most profitable channels for retaining NSs in globular clusters.

The IMF sets an upper limit to the total number of NSs that could have been formed in a cluster with some assumed initial total number of stars. For single stars with solar metallicity, the lowest initial stellar mass that yields a NS remnant is thought to be $\sim 8 M_{\odot}$. Globular clusters have a metal content that is typically $< 10\%$ of the solar value, and it is expected that the mass threshold for NS formation may be as low as $\sim 6 M_{\odot}$, but is probably not less than $\sim 5 M_{\odot}$ (e.g., Marigo, Girardi, Chiosi, & Wood 2001, and references therein). The IMF of Kroupa, Tout, & Gilmore (1993) therefore predicts that between 0.2% and 0.5% of single cluster stars should be sufficiently massive to produce NSs. If it is assumed that all massive stars are single, then a cluster that initially contains 10^6 stars should produce $\lesssim 5000$ NSs. The situation is less clear for NSs born in binary systems, owing to the effects of mass transfer.

Mass transfer in the case A and case B_e scenarios has the effect of interrupting the growth of the core of the primary, which implies a smaller final core-mass than if the primary evolved in isolation (e.g., Wellstein & Langer 1999). Consequently, the stellar mass threshold for NS formation is increased above the conventional single-star value of $8 M_{\odot}$, at least for solar metallicity. If mass transfer begins at a later stage of evolution (i.e., after central helium-burning), the final core-mass has already been established (to within $\lesssim 1 M_{\odot}$) and the mass threshold is basically unchanged. Thus, the fraction of primordial binaries that produce NS remnants is probably somewhat less than the corresponding fraction of single stars, for the same metallicity. The actual number depends on the pro-

portion of case A and case B_e systems and on the relation between the final core-mass and the evolutionary state of the primary at the time it overflows its Roche lobe.

Cases A, B, C, and D comprise roughly 5%, 25%, 25%, and 45%, respectively, of the primordial binary population. The 25% of case B systems are divided into $\sim 20\%$ case B_e and $\sim 5\%$ case B_l. Likewise, case C is comprised of $\sim 15\%$ case C_e and $\sim 10\%$ case C_l. Depending on various assumptions, any of these percentages may increase or decrease by at most roughly one-half of the values given above. It is expected that $\sim 35\%$ of the primordial binaries evolve according to the case B_e or C_e scenario; this has important implications for the retention problem.

Stable and quasi-conservative mass transfer, which is expected in a significant fraction (depending on the value of q_{crit}) of the case B_e and case C_e systems, has two notable consequences: (i) the secondary accretes much of the hydrogen-rich envelope of the primary, and (ii) the final orbital separation is typically within a factor of a few of the initial separation (see Fig. 4). The increased mass of the secondary provides a deeper gravitational potential well for the helium star, which raises the likelihood that the orbit will remain bound following the SN and hence that the NS will be retained in the cluster. The modest change in orbital separation during stable mass transfer is in sharp contrast to the dramatic shrinkage that accompanies CE evolution (see Fig. 5). For the case of small natal NS kicks, there is a clear dynamical distinction between stable and unstable mass transfer with regard to the subsequent SN explosion. As a general rule, a NS kick can be considered “small” if it is appreciably less than the relative orbital speed of the components (see Brandt & Podsiadlowski 1995).

First, consider the case of circular pre-SN orbits and *vanishing kicks*. If the binary is intact after the SN, retention in the cluster is determined by the new center-of-mass speed, v'_{CM} (e.g., Blaauw 1961; Dewey & Cordes 1987):

$$v'_{\text{CM}} = \frac{\Delta M_1}{M_b - \Delta M_1} v_1, \quad (17)$$

where ΔM_1 is the mass lost in explosion (envelope of the primary) and v_1 is the pre-SN orbital speed of the primary (helium star) about the CM. The mass M_b and the orbital speed v_1 used above correspond to the conditions immediately before the explosion, and will generally differ from their main-sequence values as a result of mass transfer. The factor that multiplies v_1 can be identified as the post-SN orbital eccentricity, e' , which gives the memorable result, $v'_{\text{CM}} = e' v_1$. Disruption of the binary must occur if the mass lost in the explosion is more than one-half of the initial systemic mass. In this case it can be shown that the speed of the liberated NS is simply equal to v_1 . Therefore, regardless of whether or not the binary is unbound following the SN, the relevant speed that determines if the NS is retained in a globular cluster is proportional to the pre-SN orbital speed of the primary.

These arguments are made more quantitative by considering a prototypical binary with a range of initial separations. Suppose this model primordial binary consists of a $10 M_\odot$ primary and a $6 M_\odot$ secondary. A typical initial orbital separation for case B_e systems is ~ 0.5 AU. Immediately after a phase of stable mass transfer, the binary will consist of the $\sim 2.2 M_\odot$ helium core of the primary

and the $\sim 10 - 14 M_\odot$ secondary, for $\beta \gtrsim 0.6$. The binary separation at this point is likely to be in the range $\sim 0.2 - 1.5$ AU (see Fig. 4), in which case the helium core has an orbital speed of $\lesssim 200 \text{ km s}^{-1}$. A spherically symmetric SN will leave the system bound, with $e' \sim 0.06$ and $v'_{\text{CM}} \lesssim 15 \text{ km s}^{-1}$. There is then a good chance that such a binary would be retained in a globular cluster. For the case of CE systems that avoid a merger (most case B_l and C_l binaries), a typical initial separation is ~ 5 AU. Following the expulsion of the CE, the essentially unaltered secondary orbits the core of the primary with a separation of $\lesssim 0.05$ AU (assuming hundred-fold decrease; see Fig. 5), giving the helium core an orbital speed of $\sim 280 \text{ km s}^{-1}$. For a $6 M_\odot$ secondary, the binary remains bound after a symmetric SN, but acquires a large recoil speed of $\sim 30 \text{ km s}^{-1}$. Thus, even in the case of small kicks, it is expected that a significant fraction of the post-CE binaries would be ejected from a typical globular cluster.

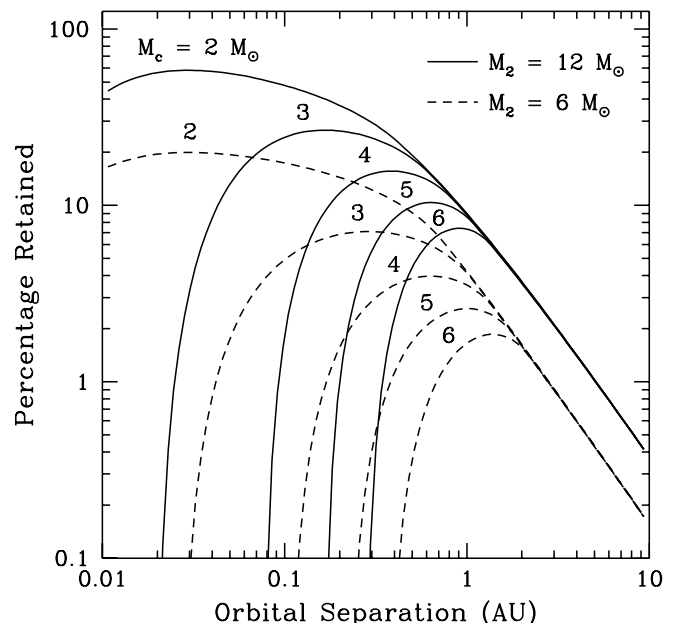


FIG. 6.— Retention probability as a function of the pre-SN orbital separation using the semianalytic formalism outlined in Appendix A. Curves are shown for secondary masses $M_2 = 12 M_\odot$ (solid) and $M_2 = 6 M_\odot$ (dashed) and five different masses, $M_c(M_\odot) = \{2, 3, 4, 5, 6\}$, of the helium star prior to the supernova explosion. We have assumed an escape speed of 50 km s^{-1} and Maxwellian kicks with $\sigma = 200 \text{ km s}^{-1}$.

We now extend this discussion and allow for a distribution in NS kick speeds. The semi-analytic formalism that we employ is described in Appendix A, and the main results are displayed in Figure 6. Figure 6 is a plot of the retained percentage of *bound* NS binaries as a function of the orbital separation immediately prior to the SN, where the escape speed is taken to be $v_{\text{esc}} = 50 \text{ km s}^{-1}$ and kick speeds are distributed as a Maxwellian with $\sigma = 200 \text{ km s}^{-1}$. The results are displayed for two different secondary masses, $M_2 = 6$ and $12 M_\odot$, which are representative values for systems that undergo dynamically unstable mass transfer and stable mass transfer, respectively. A range of helium star masses, from $M_c = 2$ to $6 M_\odot$, is also considered.

There are a number of notable features in Fig. 6. First, the retention fractions are clearly larger for $M_2 = 12 M_\odot$ and a given core mass, as expected. Also, for a given M_2 and M_c , there is a maximum retention fraction located at some value of the initial orbital separation. The fall-off at large separations results from the high characteristic kick speed relative to the comparatively low orbital speeds; many of these systems are left unbound following the SN. At sufficiently small orbital separations, which correspond to high orbital speeds, the mean CM speed of the bound post-SN binaries exceeds the cluster escape speed, and thus accounts for the decreased retention fraction at small separations. The location and height of the peak depend on the helium star mass. In light of the discussion above regarding vanishing kicks, it is clear that a more massive helium star will result in a larger dynamical perturbation to the system at the time of the SN, simply by virtue of the increased mass loss. More mass loss results in a larger fraction of the orbital speed being transformed into CM speed for a bound post-SN binary (see eq. [17]), and also raises the likelihood that the system will be disrupted if the characteristic kick speed is large. The combination of these effects explains the trends in Fig. 6, namely that, for a larger helium star mass, the height of the peak is reduced and its location shifts to larger separations (i.e., smaller orbital speeds).

If we know the typical pre-SN component masses and orbital separations among the systems that undergo stable or dynamically unstable mass transfer, Fig. 6 can be used to estimate the fraction of NSs that both remain bound to their companions following the SN and are retained in the cluster. The secondary masses used for Fig. 6 have already been appropriately chosen for this purpose. A typical helium core mass is likely to be $M_c \sim 3 M_\odot$. For the characteristic orbital separations, we chose 0.5 AU for the stable systems and 0.05 AU for the unstable systems (see discussion above). Restricting ourselves to the case B and C binaries, we should expect the ratio of stable to unstable systems to be roughly 2 : 3. Now, reading numbers directly from Fig. 6, we estimate the percentage NS binaries retained following case B or C mass transfer to be $\sim 7\%$, with $\sim 6\%$ being systems where the mass transfer was stable and the remaining $\sim 1\%$ corresponding to the unstable systems. Of course, since case B and C systems comprise only $\sim 50\%$ of the primordial binary population, the net NS retention fraction is $\sim 3.5\%$. This estimate is in accord with the results of the “standard model” discussed in the next section, where we calculate a net retention fraction of $\sim 5\%$ from all binary channels (that is, unweighted by the binary fraction among stars in the cluster).

6. NEUTRON STAR RETENTION FRACTION

6.1. Computational Procedure

We have written two versions of our population synthesis code, each with same basic engine. One version applies a given distribution in kick speeds (e.g., a Maxwellian) and a single central escape speed. With this version of the code we are able to discern which individual evolutionary pathways contribute most to the net NS retention fraction, and we can assess in a very detailed manner the influence of varying certain parameters. Only $\lesssim 10^5$ primordial binaries are sufficient to obtain reliable statistics for the ~ 70

distinct evolutionary channels followed in our code.

The second version of our code is more global; here we are interested only in the net retention fraction. A large regular grid of kick speeds and escape speeds is established. We consider a range in escape speeds from 0 to 100 km s⁻¹ and a range in kick speeds from 0 to 1000 km s⁻¹. At each position in the grid, an ensemble of binaries (typically 2×10^4) is generated and evolved. The output of the calculation is an array of retention fractions. It is then trivial to convolve the results with any of the kick distributions discussed in § 3. For each escape speed and a given kick distribution, we compute a net NS retention fraction. An example of these retention curves is shown in Figure 13. Additionally, we may also convolve the grid with a distribution of escape speeds in order to gauge the influence of a realistic cluster potential (§ 6.4).

6.2. Results

6.2.1. Maxwellian Kicks

We begin the discussion of our detailed population synthesis calculations by considering the Maxwellian kick distribution. Throughout the rest of the paper we will refer to the “standard model.” This reference model utilizes the Maxwellian kick distribution with $\sigma = 200$ km s⁻¹ and a central escape speed of $v_{\text{esc}} = 50$ km s⁻¹. The parameters that describe the primordial binary population and mass transfer for the standard model are listed in Table 3, model 5.

Distributions of the primordial binary parameters for systems that undergo case B or C mass transfer are shown in Figure 7. We have not included systems that merge following mass transfer, and hence the distribution in $\log a$ is not flat over the range shown, as would be expected from eq. 5. Furthermore, case A binaries are not included due to the small number of systems as well as the large uncertainties regarding their evolution. Figure 8 illustrates the correlation between the orbital separation and secondary mass for the systems in Fig. 7. The binaries that undergo dynamically unstable mass transfer and avoid a merger have a low mean secondary mass ($\sim 5 M_\odot$) and a large mean initial separation (~ 5 AU).

Figure 9 shows histograms of the binary parameters following mass transfer for precisely the same systems in Fig. 7. The distribution of secondary masses (sum of stable and unstable systems) shows a clear bimodality, with peaks around 5 and 12 M_\odot . This is simply a consequence of the distinction between stable and dynamically unstable mass transfer. If the mass transfer is stable, a secondary of mass $\gtrsim 4 M_\odot$ (assuming $q_{\text{crit}} \sim 2$) accretes a substantial amount of material, while the secondary mass is assumed to be unchanged if the system evolves through a CE phase. Therefore, the peak in the distribution of secondary masses for the stable systems is shifted to a higher value, and the distribution as a whole is broadened, thus reducing the height of the peak relative to the secondary mass distribution for the unstable systems. Also noteworthy is the broad peak in orbital separations (summed distribution) centered at ~ 0.1 AU, which results from the overlap of the stable and unstable systems.

A scatter plot of the secondary mass and orbital separation following mass transfer is shown in Figure 10. There is a clearly-defined boundary that marks the Roche lobe

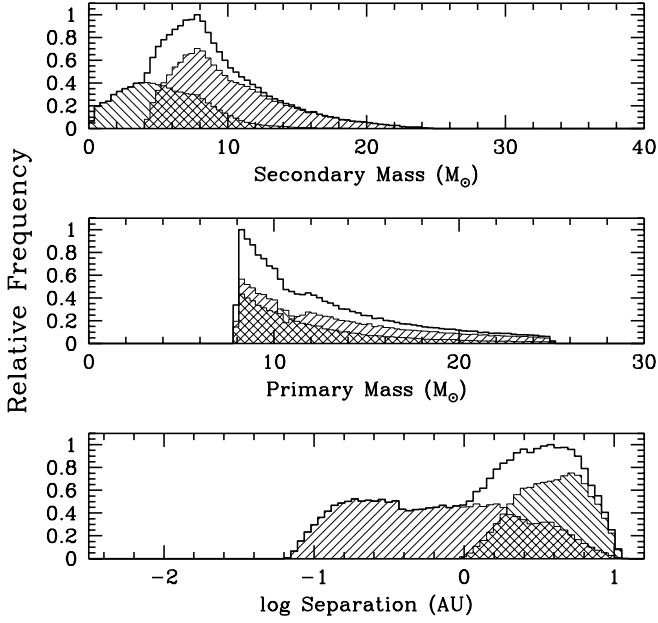


FIG. 7.— Distributions of masses and orbital separations of *primordial binaries* that undergo case B or case C mass transfer and which do not merge. Hatched regions indicate systems that undergo stable mass transfer ($+45^\circ$) and dynamically unstable mass transfer (-45°). The histogram that encloses the hatched regions is the sum of the distributions in stable and unstable systems.

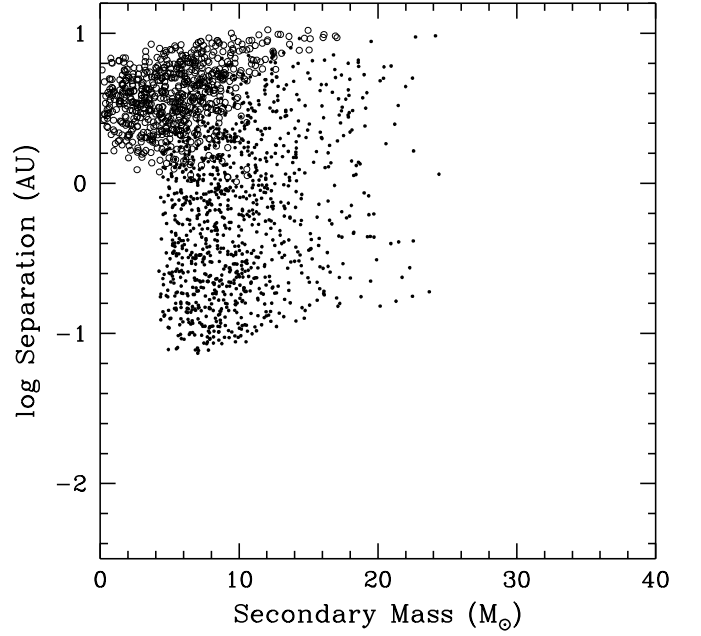


FIG. 8.— Scatter plot of circularized orbital separation versus secondary mass for the primordial binaries shown in Fig. 7. Filled and unfilled circles indicate systems that undergo stable and dynamically unstable mass transfer, respectively.

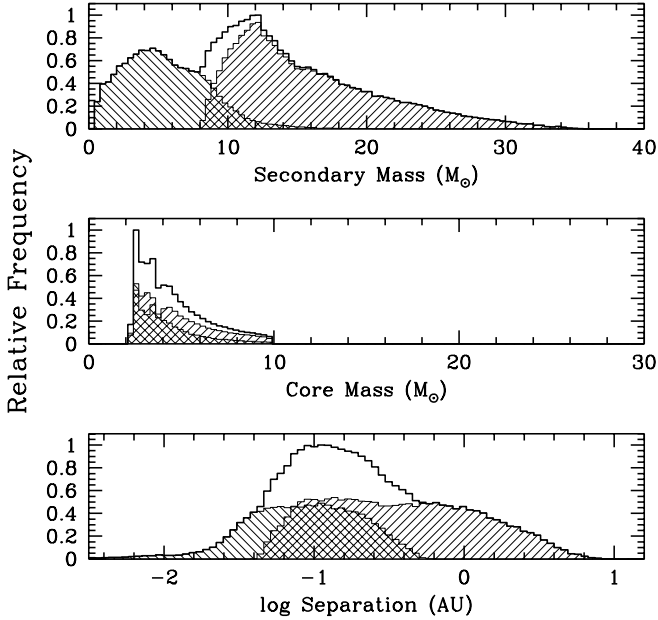


FIG. 9.— Distributions of masses and orbital parameters of systems that have undergone case B or case C mass transfer and which have not merged. The hatchings have the same meaning as in Fig. 7. These parameters indicate the state immediately prior to the supernova explosion of the helium core of the primary.

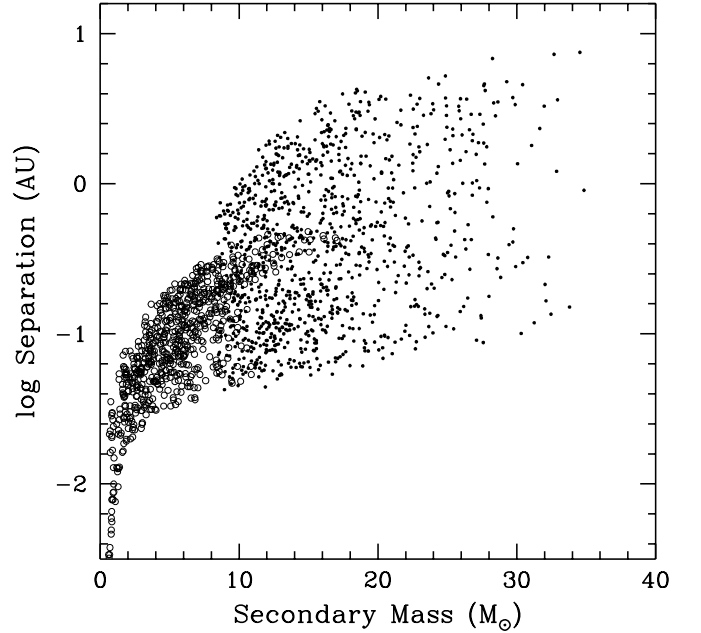


FIG. 10.— Scatter plot of separation versus secondary mass for the post-mass transfer binaries shown in Fig. 9. Note the well-defined boundary at small separations that marks the Roche lobe of the secondary. Filled and unfilled circles indicate systems that have undergone stable and dynamically unstable mass transfer, respectively.

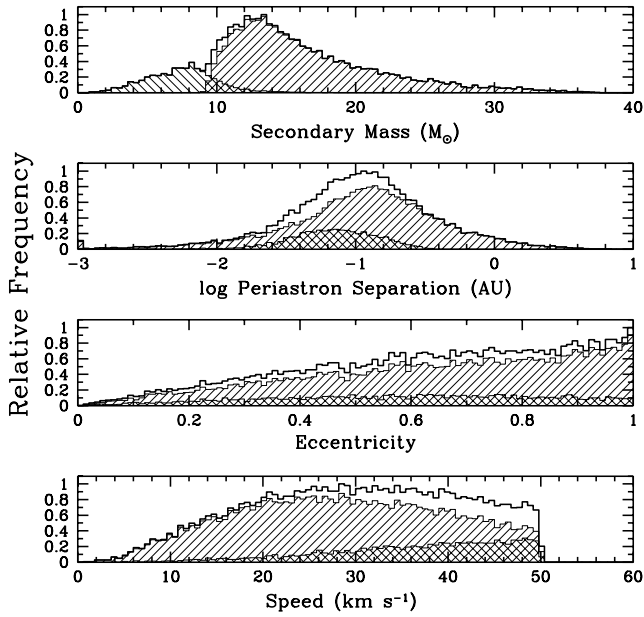


FIG. 11.— Distributions of binary parameters of systems that have undergone case B or C mass transfer, have been left bound following the supernova explosion, and have been retained in the cluster. Note that many of the systems with $\log(a/\text{AU}) \lesssim -1.3$ will experience a coalescence of the NS and the secondary immediately following the SN.

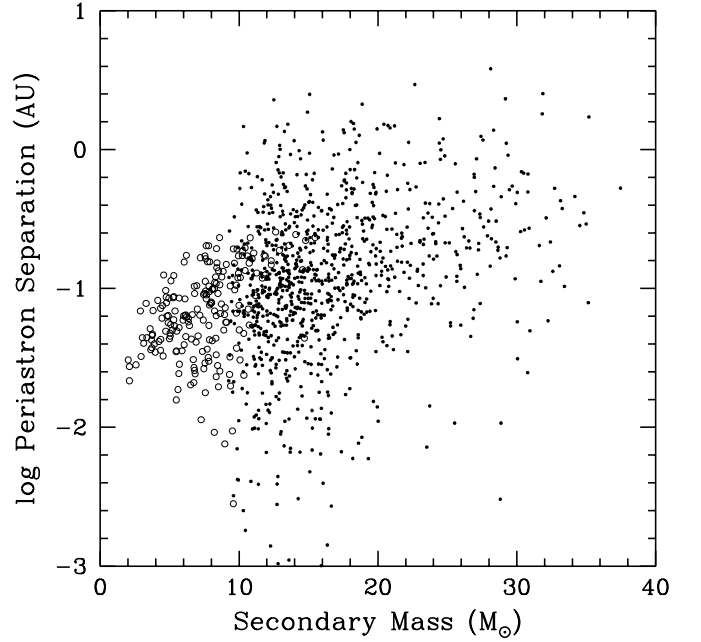


FIG. 12.— Scatter plot of periastron separation versus secondary mass for the same systems as in Fig. 11. The open and filled circles have the same meaning as in Figs. 8 and 10.

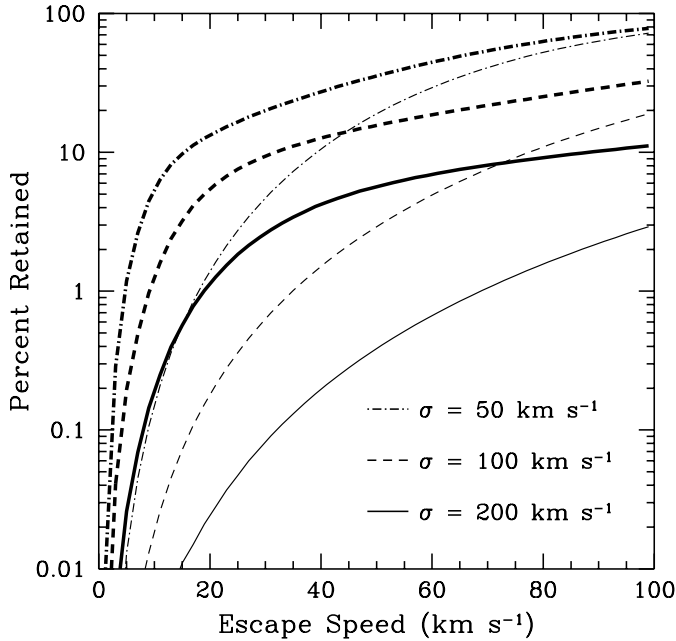


FIG. 13.— Percentage of NSs retained as a function of the cluster escape speed, for a Maxwellian distribution of kick speeds. Heavy curves correspond to binary channels, while the lighter curves are for single stars only.

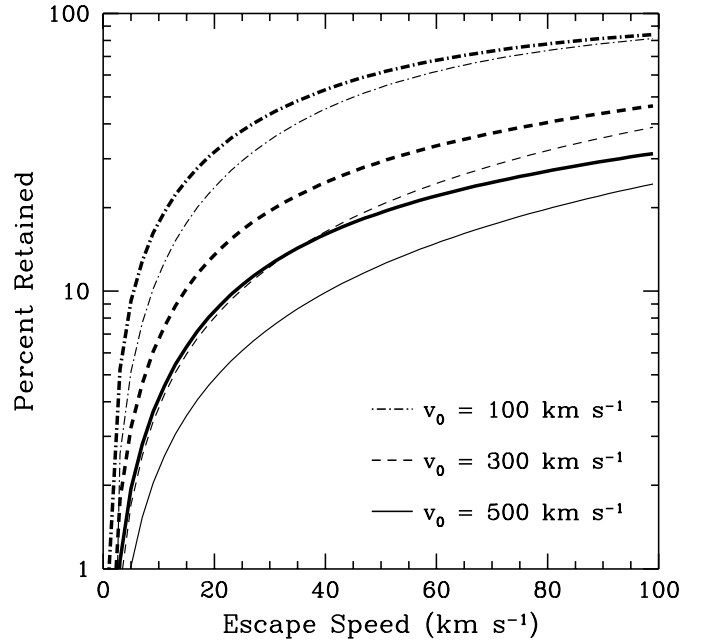


FIG. 14.— Percentage of NSs retained as a function of the cluster escape speed, for a modified Lorentzian distribution of kick speeds. Heavy curves correspond to binary channels, while the lighter curves are for single stars only.

TABLE 2
BRANCHING PERCENTAGES FOR MAXWELLIAN KICKS

Outcome	A	B _e	B _t	C _e	C _t	D
Total	5.40	21.51	3.11	15.03	6.69	48.27
Stable MT ^a	2.73	10.83	0.00	7.56	0.00	0.00
Unstable MT (CE ^b)	2.68	10.67	3.11	7.47	6.69	0.00
Merger Following MT	3.19	10.64	2.08	5.82	0.30	0.00
$\sigma = 200 \text{ km s}^{-1}$						
Unbound following SN	0.78	7.52	0.47	7.42	3.96	48.26
Bound following SN	1.43	3.34	0.56	1.78	2.44	0.01
Merger following SN	0.53	0.81	0.24	0.46	0.93	0.00
Retained single NS	0.01	0.10	0.00	0.08	0.04	0.22
Retained binary NS	0.93	2.60	0.19	0.96	0.67	0.01
Total retained	0.94	2.70	0.19	1.03	0.71	0.23
$\sigma = 100 \text{ km s}^{-1}$						
Unbound following SN	0.18	4.50	0.17	5.30	2.05	48.22
Bound following SN	2.03	6.36	0.86	3.91	4.34	0.05
Merger following SN	0.33	0.56	0.19	0.38	0.92	0.00
Retained single NS	0.01	0.27	0.01	0.31	0.09	1.54
Retained binary NS	1.52	5.71	0.63	2.90	2.46	0.05
Total retained	1.53	5.98	0.64	3.21	2.55	1.60
$\sigma = 50 \text{ km s}^{-1}$						
Unbound following SN	0.00	1.73	0.01	2.76	0.63	47.91
Bound following SN	2.20	9.13	1.02	6.45	5.77	0.36
Merger following SN	0.07	0.13	0.07	0.10	0.46	0.00
Retained single NS	0.00	0.31	0.00	0.55	0.08	9.90
Retained binary NS	1.69	8.49	0.94	5.35	4.41	0.36
Total retained	1.69	8.80	0.94	5.90	4.49	10.26

^aMT \equiv Mass Transfer.

^bCE \equiv Common-Envelope.

radius of the secondary for a given M_2 and M_c . Systems to the left of this boundary have merged following mass transfer, where the majority of merged binaries result from dynamically unstable case B_e and C_e mass transfer. From Table 2 we see that roughly one-half of the case B_e and C_e systems are expected to merge following mass transfer. This factor of one-half is a direct consequence of our choice of $q_{\text{crit}} = 1/2$. Nearly 50% more stable systems result if we set $q_{\text{crit}} = 1/4$, but additional dilution factors lead to a net retention fraction that is only $\sim 30\%$ larger – that is, ~ 1.3 times as large – when $v_{\text{esc}} = 50 \text{ km s}^{-1}$ and $\sigma = 200 \text{ km s}^{-1}$ (see Table 3).

Figures 11 and 12 show distributions relevant to the bound and retained binaries immediately following the SN that underwent case B or C mass transfer (a subset of the binaries in Figs. 7 and 9). Small periastron separations ($\lesssim 1 \text{ AU}$) among the retained NS binaries indicate that the secondaries in most of these systems, the majority of which have a mass $> 10 M_{\odot}$, will transfer material to the NS at some stage; in fact, in some cases ($\log(a/\text{AU}) \lesssim -1.3$) the radius of the secondary is larger than the periastron separation immediately after the SN, indicating an immediate coalescence. Each of these points (mass transfer and coalescence) is discussed in § 6.5. Also, note that the speed distribution of the retained binaries has significant values all the way up to the escape speed. A more realistic cluster potential and spatial distribution of stars is therefore likely to result in a marked decrease in the net retention fraction, since the fastest of the binaries in Fig. 11 would be preferentially removed from the retained pop-

ulation (see § 6.4).

Table 2 and Figure 13 are the main results of our retention study for Maxwellian kicks. The importance of case B_e and C_e systems, which contribute a large number of bound and retained binaries (see § 5), is clear in Table 2. Figure 13 shows the percentage of NSs retained in a cluster as a function of the central escape speed (applied to all stars and binaries); the curves are not weighted by the binary fraction. For $\sigma = 200 \text{ km s}^{-1}$ the retention fraction is as large as $\sim 2\%$ for single stars and $\sim 10\%$ for binaries when $v_{\text{esc}} = 100 \text{ km s}^{-1}$. It is evident from Table 2 and Fig. 13 that the retention problem is eliminated for $\sigma = 50 \text{ km s}^{-1}$, where the retained fraction of NSs with isolated progenitors is $\sim 10\%$, roughly one-half of the binary contribution.

Finally, in order to gauge how the net retention fraction changes when the free parameters of our study are modified, we have tabulated the retention fraction for a rather comprehensive set of parameters associated with the selection of primordial binaries and the behavior of mass transfer (Table 3). For Table 3, we have fixed the escape speed at $v_{\text{esc}} = 50 \text{ km s}^{-1}$ and we have utilized the Maxwellian kick distribution with $\sigma = 200 \text{ km s}^{-1}$. The largest net retention fraction of $\sim 8.3\%$ (model 9) is only a factor ~ 1.5 times larger than the retention fraction computed for the standard model (model 5). Thus, we can be secure that, for reasonable variations in the parameters listed in Table 3, the retention fraction is never much larger than the value computed for the standard model.

TABLE 3
RETENTION FRACTIONS FOR VARIOUS PARAMETER SETS

Model Number	x^a	y^b	α^c	β^d	η_{CE}^e	q_{crit}^f	Percent Retained
1	2.0	-0.5	1.5	0.75	1.0	0.50	3.23
2	2.0	0.0	1.5	0.75	1.0	0.50	5.39
3	2.0	1.0	1.5	0.75	1.0	0.50	7.87
4	2.5	-0.5	1.5	0.75	1.0	0.50	3.28
5*.....	2.5	0.0	1.5	0.75	1.0	0.50	5.79
6	2.5	1.0	1.5	0.75	1.0	0.50	8.03
7	3.0	-0.5	1.5	0.75	1.0	0.50	3.41
8	3.0	0.0	1.5	0.75	1.0	0.50	5.71
9	3.0	1.0	1.5	0.75	1.0	0.50	8.27
10	2.5	0.0	1.0	0.25	0.3	0.50	3.70
11	2.5	0.0	1.0	0.25	1.0	0.50	4.12
12	2.5	0.0	1.0	0.75	0.3	0.50	4.20
13	2.5	0.0	1.0	0.75	1.0	0.50	3.70
14	2.5	0.0	1.0	1.00	0.3	0.50	2.94
15	2.5	0.0	1.0	1.00	1.0	0.50	3.32
16	2.5	0.0	1.5	0.25	0.3	0.50	2.23
17	2.5	0.0	1.5	0.25	1.0	0.50	2.63
18	2.5	0.0	1.5	0.75	0.3	0.50	5.15
19	2.5	0.0	1.5	1.00	0.3	0.50	2.94
20	2.5	0.0	1.5	1.00	1.0	0.50	3.32
21	2.5	0.0	2.0	0.25	0.3	0.50	0.72
22	2.5	0.0	2.0	0.25	1.0	0.50	1.15
23	2.5	0.0	2.0	0.75	0.3	0.50	5.54
24	2.5	0.0	2.0	0.75	1.0	0.50	5.93
25	2.5	0.0	2.0	1.00	0.3	0.50	2.94
26	2.5	0.0	2.0	1.00	1.0	0.50	3.32
27	2.5	0.0	1.5	0.75	1.0	0.25	7.06
28	2.5	0.0	1.5	0.75	1.0	0.75	3.38

*Standard model.

^aIMF exponent.

^bExponent for mass ratio distribution.

^cAngular momentum-loss parameter.

^dMass capture fraction.

^eCommon-envelope efficiency.

^fCritical mass ratio that separates stable and unstable mass transfer when the secondary is radiative.

6.3. Modified Lorentzian Kicks

We now repeat the exercise of the last section, but with the modified Lorentzian kick distribution proposed by Paczyński (1990). The qualitative feature of Paczyński's distribution that distinguishes it from the Maxwellian is its finite value at vanishing kick speeds. Physically speaking, this feature is unrealistic, since various stochastic processes associated with core-collapse and the SN explosion are certain to deliver some net impulse to the newly formed NS; the characteristic *minimum* kick speed is likely to be of order 10 km s^{-1} rather than, say, 10 m s^{-1} . However, the possibility that some finite fraction of NSs receive kicks between 10 and 50 km s^{-1} is not necessarily unrealistic.

Table 4 summarizes the results of applying the modified Lorentzian distribution, for $v_{\text{esc}} = 50 \text{ km s}^{-1}$ and $v_0 (\text{km s}^{-1}) = \{100, 300, 500\}$. Of particular significance is the large fraction of NSs born in case D binaries that are retained in the cluster ($\sim 6\%$ for $v_0 = 500 \text{ km s}^{-1}$). This simply indicates that the Paczyński distribution, even with a large mean speed, allows a high percentage of the NSs born in isolation to be retained in a cluster. In fact, for the values of v_0 used to generate Table 4, the retention fraction of single NSs dominates over the contribution from any of

the other five cases of mass transfer. Figure 14 illustrates this point clearly; the percentage of NSs retained via binary channels is never more than a factor of two over the retained percentage of NSs born from isolated progenitors.

6.4. Spatial Distribution and the Cluster Potential

Up to this point we have discussed those calculations where the nominal central escape speed has been applied to all stars and binaries in question. The combination of competitive gas accretion processes, stellar collisions, and dynamical mass segregation in the early phases of cluster development and star formation may lead to a centrally concentrated population of massive stars (see Bonnell, Bate, & Zinnecker 1998). However, the spatial distribution would certainly have been finite and the same escape speed would not have applied to all stars. We investigate the possibility that massive stars and binaries are born within a finite spherical volume, with a gravitational potential that is appropriate for a young globular cluster.

For simplicity, we suppose that all massive single stars and binaries are distributed uniformly within a spherical volume of radius R about the center of the cluster. Thus, the probability that an object is located within a spherical shell of radius r and thickness dr is simply

$$p(r) dr = \frac{3r^2 dr}{R^3}. \quad (18)$$

Furthermore, at the time of the SN explosion, we assume that the single star or binary is at rest. This is reasonable, since it is expected that the characteristic speed of these massive objects is $\lesssim 5 \text{ km s}^{-1}$.

The background of lower-mass objects in the cluster provides the net gravitational potential well in which the massive stars reside. This assumes that all the cluster stars were formed at essentially the same time or that the low-mass stars formed first. We adopt a Plummer model for the potential (e.g., Binney & Tremaine 1987), given by

$$\Phi = -\frac{GM_*}{(r^2 + b^2)^{1/2}}, \quad (19)$$

where M_* is the total mass in background stars, r is the distance from the cluster center, and b is the “core” radius of the model. In dynamical models of globular cluster evolution that include the effects of tidal mass loss, it is often assumed that any star that crosses a sphere of radius r_t (the tidal radius) is lost from the cluster (e.g., Joshi, Nave, & Rasio 2001, and references therein). The tidal radius is a function of position in the Galaxy; at a few kiloparsecs from the Galactic center, r_t is of order 100 pc for a $10^6 M_\odot$ cluster. The escape speed, $v_{\text{esc}}(r)$, at a radius r is obtained from the energy relation

$$\frac{1}{2}v_{\text{esc}}^2(r) = \Phi(r_t) - \Phi(r). \quad (20)$$

However, for the purposes of this investigation we assume that r_t is sufficiently large in comparison to any relevant radius in the cluster that we may drop $\Phi(r_t)$, so that $v_{\text{esc}}^2(r) = -2\Phi(r)$. In this case, the core radius, b , is a simple function of the central escape speed, $v_{\text{esc}}(0)$:

$$b = \frac{2GM_*}{v_{\text{esc}}^2(0)}. \quad (21)$$

The output of our population synthesis code is a two-dimensional grid of retention fractions as a function of the

TABLE 4
BRANCHING PERCENTAGES FOR MODIFIED LORENTZIAN KICKS

Outcome	A	B _e	B _t	C _e	C _t	D
Total	5.43	21.44	2.96	15.30	6.76	48.11
Stable MT ^a	2.70	10.78	0.00	7.76	0.00	0.00
Unstable MT (CE ^b)	2.73	10.66	2.96	7.54	6.76	0.00
Merger Following MT	3.22	10.64	1.94	5.86	0.33	0.00
$v_0 = 500 \text{ km s}^{-1}$						
Unbound following SN	0.67	5.78	0.38	6.06	3.12	47.09
Bound following SN	1.53	5.02	0.65	3.39	3.31	1.02
Merger following SN	0.33	0.52	0.16	0.30	0.73	0.00
Retained single NS	0.00	0.12	0.00	0.21	0.05	5.23
Retained binary NS	1.06	4.29	0.44	2.51	1.81	1.02
Total retained	1.06	4.40	0.45	2.71	1.86	6.25
$v_0 = 300 \text{ km s}^{-1}$						
Unbound following SN	0.36	4.17	0.22	4.73	2.10	46.46
Bound following SN	1.84	6.63	0.81	4.71	4.33	1.66
Merger following SN	0.25	0.48	0.16	0.25	0.71	0.00
Retained single NS	0.01	0.19	0.00	0.24	0.05	8.61
Retained binary NS	1.36	5.90	0.63	3.69	2.66	1.66
Total retained	1.37	6.09	0.63	3.93	2.71	10.26
$v_0 = 100 \text{ km s}^{-1}$						
Unbound following SN	0.04	1.24	0.03	1.91	0.52	43.35
Bound following SN	2.16	9.57	1.00	7.53	5.91	4.76
Merger following SN	0.06	0.14	0.05	0.08	0.47	0.00
Retained single NS	0.00	0.19	0.00	0.43	0.04	22.00
Retained binary NS	1.66	8.87	0.93	6.35	4.52	4.76
Total retained	1.67	9.07	0.93	6.78	4.56	26.76

^aMT \equiv Mass Transfer.

^bCE \equiv Common-Envelope.

escape speed and the kick speed (see § 6.1). Combining eqs. (18), (19), and (20; dropping $\Phi(r_t)$), we obtain a distribution in escape speeds for the spherical distribution of massive stars,

$$p(u_{\text{esc}}) du_{\text{esc}} = 6 \left(\frac{b}{R} \right)^3 u_{\text{esc}}^{-7} (1 - u_{\text{esc}}^4)^{1/2} du_{\text{esc}}, \quad (22)$$

where $u_{\text{esc}} \equiv v_{\text{esc}}/v_{\text{esc}}(0)$ is a dimensionless escape speed.

It is a simple matter to convolve the grid of retention fractions with both the distribution of kick speeds and the distribution of escape speeds to obtain a net retention fraction, as a function of $v_{\text{esc}}(0)$ and R . We have tabulated (Table 5) the net retention fraction for different values of $v_{\text{esc}}(0)$ and R using the Maxwellian kick distribution with $\sigma = 200 \text{ km s}^{-1}$ and a cluster mass of $M_* = 10^6$. For $v_{\text{esc}}(0) = 50 \text{ km s}^{-1}$ and $R = 20 \text{ pc}$, the percentage of NS retained in the cluster is reduced by a factor of ~ 3 below the standard model value of $\sim 5.6\%$ (see Table 3). Thus, a realistic cluster potential and finite spatial distribution of stars is indeed an important consideration.

6.5. Binary Evolution After the First Supernova

The standard model (§ 6.2.1) has a very striking feature: massive secondaries ($M_2 \gtrsim 10 M_\odot$) are prevalent among the retained binaries following the first SN (see Figs. 11 and 12). The majority of these massive systems have periastron separations $\lesssim 1 \text{ AU}$, which implies that most of the secondaries will begin to transfer material to the NS at some point. Furthermore, the extreme mass ratios suggest that the mass transfer will be dynamically unstable,

resulting in a spiral-in of the NS into the envelope of the secondary. It should be noted that the evolution of the secondary following mass transfer may not precisely resemble the evolution of an isolated star of the same mass (e.g., Braun & Langer 1995; Wellstein, Langer, & Braun 2001); in fact, the evolution may be qualitatively different.

Before we discuss the possible outcomes of the spiral-in, we mention an important caveat. Extreme accretion rates ($> 10^{-4} M_\odot \text{ yr}^{-1}$) onto the NS – rates far exceeding the standard, radiative Eddington limit of $\sim 10^{-8} M_\odot \text{ yr}^{-1}$ – may be possible if the gravitational energy is lost to neutrinos (e.g., Chevalier 1993, 1996; Fryer, Benz, & Herant 1996; Brown, Lee, & Bethe 2000). If this “hypercritical accretion” occurs while the NS spirals into the envelope of a massive secondary, it is likely that the NS will collapse into a black hole, although the three-dimensional nature of the hydrodynamical problem implies that this process is very uncertain. Obviously, this outcome is not desirable in regard to the retention problem, since a NS is lost if it is transformed into a black hole. We now proceed under the assumption that the NS does not undergo hypercritical accretion during the spiral-in phase; however, the NS may still collapse to a black hole at a later stage.

The envelope of the massive secondary may be successfully ejected if the circularized orbital separation is $\gtrsim 1 \text{ AU}$ (see Taam, Bodenheimer, & Ostriker 1978). This applies to only a few percent of the systems in Figs. 11 and 12. If the envelope is ejected, and the helium core of the secondary is exposed, the formation of a second NS is possible. However, the eventual SN explosion of the helium star

TABLE 5
MODIFIED RETENTION FRACTIONS FOR A FINITE SPATIAL DISTRIBUTION OF STARS

$v_{\text{esc}}(0)$ (km s ⁻¹)	R (pc)	b (pc)	Percent Retained	Reduction Factor*
30	5	9.88	2.44	0.94
30	10	9.88	2.10	0.81
30	20	9.88	1.47	0.56
50	5	3.56	4.44	0.79
50	10	3.56	3.12	0.55
50	20	3.56	1.81	0.32
70	5	1.81	5.19	0.64
70	10	1.81	3.38	0.42
70	20	1.81	1.87	0.23

*Factor by which retention fraction is reduced
below value obtained with $R = 0$ pc.

is likely to send the first- and second-formed NSs speeding out of the cluster, even if the kick to the second NS is small and the binary remains bound after the explosion (see § 5).

The much more likely outcome among the retained NS binaries is a complete coalescence of the NS and the massive secondary, resulting in the formation of a Thorne-Żytkow object (TŻO; Thorne & Żytkow 1975, 1977; Biehle 1991; Cannon 1993; Podsiadlowski, Cannon, & Rees 1995), where hydrostatic support is provided by gravitational energy release or exotic nuclear burning processes near the surface of the NS. The ultimate fate of the NS is unclear. If the NS survives, it will probably emerge as a rapidly rotating object with the slow speed of the retained post-SN binary. However, it is possible, and perhaps likely, that the NS will collapse into a black hole during the late stage of massive TŻO evolution (Podsiadlowski, Cannon, & Rees 1995; Fryer, Benz, & Herant 1996).

In addition to the high-mass systems in Figs. 11 and 12, roughly 10% of the retained binaries have low- to intermediate-mass secondaries ($M_2 \lesssim 8 M_\odot$), all of which are the product of dynamically unstable mass transfer prior to the SN. Mass transfer onto the NS in the circularized binary is likely to be dynamically unstable for $M_2 \gtrsim 4 M_\odot$ (Podsiadlowski, Rappaport, & Pfahl 2001), while for secondaries of lower mass the system will exist for some time as a low- or intermediate-mass X-ray binary, which may ultimately yield a millisecond radio pulsar with a very low-mass companion.

7. CONCLUSIONS

The NS retention fraction calculated within our standard model is $\sim 5\%$ for NSs born in binary systems. Reasonable variations of the parameters that describe the primordial binary population and binary evolution during mass transfer give a retained percentage between ~ 1 and 8% (Table 3). If we distribute the massive binaries within a sphere of some finite radius and embed the population in a realistic background gravitational potential, the retention fraction may be reduced by a factor of $\sim 2 - 3$ (Table 5). If we suppose that one-half of the massive stars in a young cluster are in binaries, then the retention fraction is further reduced by a factor of two. Therefore, a more realistic net retention fraction is probably of order 1% , when we apply the Maxwellian kick distribution with $\sigma = 200 \text{ km s}^{-1}$.

As compared to the contribution from single stars, binary systems do provide a much more efficient channel for retaining NSs when the characteristic kick speed is large. However, it appears the net NS retention fraction may not be sufficient to explain the abundance of NSs in globular clusters. In fact, even if as many as 10^4 NSs are formed out of 10^6 stars, our standard model, combined with the binary fraction and realistic cluster potential, predicts that only 100 NSs could have been retained. It is unlikely that such a small number of NSs is compatible with what is observed in certain clusters (e.g., 47 Tuc). We suggest that binaries alone do not provide a robust solution to the retention problem, and we now discuss alternative hypotheses.

8. DISCUSSION

Our standard model for the formation and retention of NS in globular clusters predicts a retention fraction of $\sim 5\%$. Additional layers of realism, including a finite spatial distribution of stars embedded in a background cluster potential, and a binary fraction of massive stars, may reduce this number by more than a factor of four. We suggest that our standard model requires significant modification in order for the results to be consistent with observations. Here, we briefly speculate on possible alternative solutions to the retention problem.

8.1. The Kick Distribution

A very simple “fix” to the retention problem is to assume that the true underlying distribution in NS kicks has a much lower mean speed than the Galactic pulsars suggest. Such a distribution would require a substantial number of slowly-moving pulsars, which, for some reason, have not yet been detected. Maybe the pulsar sample is too small, or perhaps some systematic effect is unaccounted for in studies of pulsar kinematics, or both. A complete consistency check is difficult, if not impossible, and must incorporate all of the uncertain theory of single star and binary stellar evolution. In addition, we require some rudimentary understanding of the physical mechanism that produces the largest NS kicks. One possibility is that small kicks preferentially occur in binary systems, in which case the associated NS is likely to remain bound to its companion following the SN and thus will not appear as an isolated pulsar.

8.2. Implications of Wide, Nearly Circular High-Mass X-ray Binaries

Recently, a new class of high-mass X-ray binaries (HMXBs) has emerged. These systems exhibit relatively low eccentricities ($e \lesssim 0.2$) and orbital periods sufficiently long ($P_{\text{orb}} \gtrsim 100$ d) that tidal circularization could not have played a significant role. A detailed analysis of one such system (X Per/4U 0352+30; Delgado-Martí et al. 2001) revealed that the observed orbit is entirely consistent with the NS having been born with no kick whatsoever. Table 6 lists names and orbital parameters of systems that belong to the class of wide, nearly circular HMXBs.

It is interesting to note that the present orbit of XTE J1543-568 (in 't Zand, Corbet, & Marshall 2001) is not precisely consistent with both zero kick and a perfectly circular pre-SN orbit; the eccentricity is too small by a factor of 2–3. One or the other assumption must be relaxed. If we demand that the pre-SN orbit was circular, then it is straightforward to show that a very small kick of $< 10 \text{ km s}^{-1}$ is required to produce the observed eccentricity, and that the direction of the kick does not have to be finely tuned.

With some perspective, we can motivate a phenomenological picture that accounts for the population of wide, nearly circular HMXBs, and which is consistent with what we know about the Galactic NS population. Our model must satisfy three basic constraints. First, the systems listed in Table 6 are quite wide and thus have not experienced the dramatic orbital shrinkage associated with dynamically unstable mass transfer; the mass transfer in these systems was likely in accord with the stable case B_e or C_e scenario described in § 4.2. We propose that a significant fraction of those NSs whose progenitors underwent case B_e or C_e mass transfer received only a small kick (e.g., $\lesssim 50 \text{ km s}^{-1}$). Second, the model should be able to approximately reproduce the numbers and properties of the observed population of bright low-mass X-ray binaries (LMXBs) in the Galaxy. Third, our basic picture should also be consistent with the observed kinematical distribution of isolated pulsars in the Galaxy, on which the NS kick distributions are based. These latter two constraints are satisfied if we suppose that a NS received the usual large kick if its progenitor was allowed to evolve into a red supergiant (i.e., a single progenitor or case B_l , C_l , or D for a binary system). The standard formation channel for LMXBs involves a common-envelope phase in the case B_l or C_l scenario (e.g., Kalogera & Webbink 1998), and so the NSs in these systems would have received the conventional large kicks by our hypothesis. Also, within this framework, isolated, fast-moving pulsars are likely to have come from single progenitors or wide binaries that were disrupted owing to the SN.

We repeated the retention study with the following assumptions regarding NS kicks. If the orbit of the primordial binary is sufficiently wide that mass transfer begins when the star is a red supergiant (i.e., case B_l , C_l , or D), the NS kick is chosen from a Maxwellian distribution with $\sigma = 200 \text{ km s}^{-1}$, as in the standard model (see § 6.2.1). However, if the mass transfer is stable and case B_e or C_e , we utilize a Maxwellian kick distribution with $\sigma = 10 \text{ km s}^{-1}$. Using the standard-model parameters given in Table 3, model 5, we calculate a net retention

fraction contributed by binary channels of $\sim 20\%$. Therefore, we see that the above scenario greatly reduces the severity of the retention problem. Figure 15 shows the distributions in orbital parameters and speeds for the retained NS binaries. On average, the systems in Fig. 15 are wider, more circular, and are moving more slowly than the systems in Fig. 11, which shows the same distributions, but for the standard model.

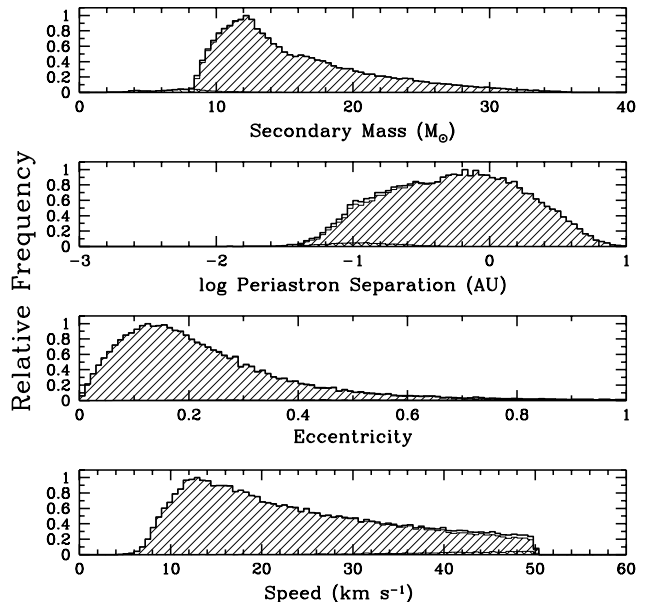


FIG. 15.— Distributions of binary parameters of systems that have undergone case B or C mass transfer, have been left bound following the supernova explosion, and have been retained in the cluster, where we have assumed that case B_e and C_e receive kicks drawn from a Maxwellian with $\sigma = 10 \text{ km s}^{-1}$. Compare this figure to Fig. 11.

There is a plausible physical argument that may support the empirically-motivated phenomenological hypothesis outlined above. Young, isolated, massive stars are observed to rotate at $\sim 20 - 50\%$ of their breakup rates (e.g., Fukuda 1982). During the hydrogen-burning main sequence, the structure of the star changes sufficiently slowly that various hydrodynamical and magnetohydrodynamical processes should be effective in enforcing nearly uniform rotation throughout much of the star (Spruit & Phinney 1998; Heger, Langer, & Woosley 2000). Immediately following the depletion of hydrogen in the core, the structure of the star changes dramatically; the envelope expands to giant dimensions on a thermal timescale ($\sim 10^3 - 10^4$ yr) and the core contracts while conserving angular momentum. If the helium core is exposed during this rapid expansion phase as a result of mass transfer in a binary system (case B_e or possibly C_e ; see Figs. 2 and 3), the nascent helium star is likely to be rapidly rotating. On the other hand, if the star is allowed to evolve into a red supergiant, Maxwell stresses may strongly couple the mostly convective and very slowly rotating envelope to the core, causing the core to spin down to the angular velocity of the envelope (Spruit & Phinney 1998; Spruit 1998).

This argument suggests a possible dichotomy in core-collapse dynamics between isolated stars and some stars born in close binary systems. It may be that a helium core

TABLE 6
ORBITAL PARAMETERS FOR NEARLY CIRCULAR HIGH-MASS X-RAY BINARIES

Object	$P_{\text{orb}}(\text{days})$	e	$f_X(M)(M_\odot)^a$	Reference
X Per/4U 0352+30 ..	249.90 ± 0.50	0.111 ± 0.018	1.61 ± 0.06	Delgado-Martí et al. 2001
γ Cas ^b	203.59 ± 0.29	0.260 ± 0.035	...	Harmanec et al. 2001
XTE J1543-568	75.56 ± 0.25	< 0.03	8.2 ± 0.5	in 't Zand, Corbet, & Marshall 2001
2S 1553-542 ^c	30.60 ± 2.20	< 0.09	5.0 ± 2.1	Kelley, Rappaport, & Ayasli 1983
GS 0834-430	105.80 ± 0.40	$\lesssim 0.17$	0.2 ± 0.3	Wilson et al. 1997

^aMass function from X-ray timing.

^bOrbital parameters determined from optical light curve.

^cThis orbital period is sufficiently short that tidal interactions may have circularized the orbit somewhat (Kelley, Rappaport, Ayasli 1983).

exposed following case B_e or C_e mass transfer is rotating much faster than the core of an isolated star at a late stage of its evolution. Dynamically, the collapse of a rapidly rotating core is certainly more phenomenologically complex than the collapse of an initially static core. However, it is not obvious a priori whether a rapidly rotating or slowly rotating core should ultimately yield a larger average natal kick to the NS. Perhaps the rotation axis provides a preferred direction for the escape of neutrinos or the formation of jets and the NS receives a kick perpendicular to the orbital plane. Another possibility is that rapid rotation stalls the collapse somewhat (e.g., Fryer & Heger 2000), allowing many rotations before the NS is formed. A large number of rotations of the collapsing core may have the effect of averaging out the asymmetries that give rise to large NS kicks (Spruit & Phinney 1998). These speculations aside, we are motivated by empirical evidence to suggest that helium stars exposed following stable case B_e or (possibly) C_e mass transfer produce NSs with small natal kicks, while NSs formed following mass transfer at a later stage of evolution may receive the conventional large kicks.

8.3. Accretion-Induced Collapse

Thus far, we have considered only massive stellar progenitors of NSs. However, if the mass of a white dwarf can be increased to the critical Chandrasekhar value ($\simeq 1.4 M_\odot$), the white dwarf may collapse to form a NS. This *accretion-induced collapse* (AIC) scenario was proposed by Grindlay (1987; see also Bailyn & Grindlay 1990) in the context of globular clusters to explain a number of things regarding cluster NS populations, the retention problem among them. Two fundamentally different scenarios have been proposed for the formation of a NS via AIC, which we now discuss in turn.

A white dwarf may be “grown” to the Chandrasekhar mass by the slow accumulation of material accreted from a stellar companion. In this scenario, if the white dwarf has a C/O composition it is more likely to explode in a Type Ia SN, than to collapse to form a neutron star (e.g., Nomoto 1987; Rappaport, DiStefano, & Smith 1994). More favorable candidates for AIC are white dwarfs with an O/Ne/Mg composition (e.g., Nomoto 1987; Nomoto & Kondo 1991). These are relatively rare white dwarfs with masses above $\sim 1.2 M_\odot$. To grow the white dwarf to the Chandrasekhar mass, however, requires some fine tuning in the accretion rate, which must lie in the relatively narrow range of about $3 - 7 \times 10^{-7} M_\odot \text{ yr}^{-1}$ (Iben 1982;

Nomoto 1982; Rappaport, DiStefano, & Smith 1994). For significantly lower accretion rates, the burning of hydrogen to helium is likely to be unstable, leading to hydrodynamical nova explosions, which may eject at least as much mass as was accreted (e.g., Prialnik & Kovetz 1995). For larger transfer rates the white dwarf atmosphere will tend to swell to giant dimensions and may overflow its Roche lobe, thereby losing much of the accreted matter. Perhaps the most promising cases for obtaining mass transfer rates within the above narrow range occur for thermal timescale mass transfer via the Roche lobe overflow in binaries with relatively unevolved companions in the mass range $1.5 - 2.5 M_\odot$ (e.g., supersoft X-ray sources; van den Heuvel et al. 1992; Rappaport, DiStefano, & Smith 1994). Another possibility occurs for the case of accretion from the strong stellar wind of a low-mass giant (Iben & Tutukov 1984; Hachisu, Kato, & Nomoto 1999).

A second possible AIC channel involves the coalescence of two white dwarfs (e.g., Nomoto 1987; Chen & Leonard 1993; Rasio & Shapiro 1995). Two white dwarfs in a close binary system will be drawn together as gravitational radiation removes orbital angular momentum. The negative mass-radius exponent of a white dwarf implies that the less massive component will first fill its Roche lobe. Like the standard AIC scenario, which involves only one white dwarf, the double white dwarf merger model has been proposed as an evolutionary pathway to the formation of Type Ia SNe (e.g., Iben & Tutukov 1984; Webbink 1984; Saffer, Livio, & Yungelson 1998, and references therein); however, it is now considered more likely that this will lead to disruption of the lighter white dwarf (see Nomoto & Iben 1985). Under the assumption that the merger does not produce a Type Ia SN, in order for the double white dwarf system to ultimately yield a NS, the sum of the masses must exceed the Chandrasekhar mass. Approximately 1 out of every 1000 primordial binaries should produce such a massive double white dwarf close enough to merge within a Hubble time (e.g., Han 1998; Nelemans et al. 2001). If a sizable fraction of these systems can collapse to form a NS, rather than explode as a Type Ia SN, then perhaps as many as 1000 NSs can be formed in this way in a globular cluster. However, binary population synthesis in a globular cluster is substantially more complex than in the Galactic plane, owing to the dynamical interactions among binaries and single stars.

We have not attempted to follow any of these channels in this work. This would certainly be a worthwhile future study to help quantify the formation rates of NSs via AIC

in both globular clusters and in the Galactic plane. Finally, we note that there is no obvious reason why a NS formed via AIC would be less subject to the same type of accelerations as those formed from collapsed cores of massive stars, especially if the NS velocities are acquired as a result of asymmetric neutrino emission or the post-natal electromagnetic rocket mechanism (Harrison & Tademaru 1975; see also Lai, Chernoff, & Cordes 2001).

8.4. Supermassive Globular Clusters

Tidal stripping of globular clusters is a theoretically well-studied phenomenon (e.g., Chernoff & Weinberg 1990; Takahashi & Portegies Zwart 2000; Joshi, Nave, & Rasio 2001). It has been shown (see Joshi, Nave, & Rasio for a recent discussion) that, for a range in parameters that describe the initial cluster equilibrium model, a cluster may disrupt in the tidal field of the Galaxy in less than 10^{10} yr, owing to the combined effects of mass loss during stellar evolution and the diffusion of stars across the cluster's tidal boundary (effectively, its Roche lobe). The survivability of a cluster depends on its location in the Galaxy, its central concentration, and on the shape of the cluster IMF (in particular, the slope of the IMF above $\sim 2 M_\odot$). Clusters with a high central concentration and a small proportion of massive stars are more likely to survive to core collapse, although as much as 90% of the initial mass of the cluster may be lost before this phase is reached (Joshi, Nave, & Rasio 2001).

The idea that a cluster may lose a very significant fraction of its mass, but still “survive” in some sense, brings to light the interesting and very real possibility that some

of the globular clusters that presently have a mass of $\sim 10^6 M_\odot$ are, in fact, remnants of clusters with an initial mass in stars of $\gtrsim 10^7 M_\odot$. At least one such supermassive cluster has been discovered in the Andromeda galaxy (Meylan et al. 2001), and it has been speculated that this cluster is actually the core of a dwarf elliptical galaxy. For a cluster of initial mass $10^7 M_\odot$, a net NS retention fraction of a few percent, along with a standard IMF, implies possibly a thousand NSs at the current epoch, which may be sufficient to explain the present pulsar and X-ray binary populations in globular clusters.

We are not the first to consider this rather extreme possibility. Motivated by the hundred-fold overabundance (per unit mass) of bright X-ray sources in globular clusters relative to the Galactic disk, Katz (1983) suggested that perhaps some clusters lose all but $\sim 1\%$ of their mass through evaporative processes. Although it is now believed that 3- and 4-body dynamical scenarios (e.g., Rasio, Pfahl, & Rappaport 2000), and perhaps tidal capture (e.g., Fabian, Pringle, & Rees 1975; DiStefano & Rappaport 1992; Podsiadlowski, Rappaport, & Pfahl 2001), can explain the overabundance of X-ray binaries, excessive mass loss from initially supermassive globular clusters is still an interesting possibility for explaining the large numbers of NSs found in clusters today.

EP would like to acknowledge the hospitality of Oxford University, where some of this work was initiated. We thank Fred Rasio for many stimulating discussions on the topic of globular clusters. This work was supported in part by NASA ATP grant NAG5-8368.

APPENDIX

A. ESTIMATE OF THE BINARY RETENTION FRACTION

A semi-analytic approach is used to compute the probability that a binary is bound following the SN explosion *and* is retained in a cluster with a given escape speed. For an appropriate choice of pre-SN orbital separation and component masses, the calculated retention probability is a fair estimate of the net NS retention fraction contributed by all binary stellar evolution channels (see § 5).

In what follows, we consider a circular pre-SN binary of total mass M_b and with separation a , so that the relative orbital speed is $v_{\text{orb}} = (GM_b/a)^{1/2}$. We assume that the explosion is instantaneous and leaves a neutron star remnant of mass M_{NS} . Furthermore, we neglect the effect of the SN ejecta on the secondary. The kick speed imparted to the NS is v_k and the systemic mass after the explosion is M'_b .

It is useful here to introduce a set of dimensionless variables. All speeds are expressed in units of the pre-SN relative orbital speed, v_{orb} , and are denoted by the variable w with an appropriate subscript (e.g., $w_k \equiv v_k/v_{\text{orb}}$ is the dimensionless kick speed). The fractional mass loss in the explosion is given by $\Delta \equiv 1 - M'_b/M_b$. In place of the secondary mass M_2 , we use the post-SN mass ratio $q' \equiv M_2/M_{\text{NS}}$. Finally, the variable u represents the cosine of the angle between the direction of the kick and the direction of the pre-SN relative orbital velocity; note $u = 0$ when the kick is directed perpendicular to the orbital plane.

The orbital energy, E' , of the post-SN binary is proportional to the dimensionless quantity (e.g., Hills 1983; Brandt & Podsiadlowski 1995)

$$E' \propto -1 + 2\Delta + w_k^2 + 2u w_k. \quad (\text{A1})$$

For the purposes of § 5 it is sufficient to consider $\Delta < 1/2$, in which case there is a minimum kick, $w_{k,\text{min}}$, required to unbind the system, realized when $u = 1$:

$$w_{k,\text{min}} = -1 + [2(1 - \Delta)]^{1/2}. \quad (\text{A2})$$

Likewise, for there to be a finite probability that the system remains bound, w_k must be less than some large value, $w_{k,\text{max}}$, corresponding to $E' = 0$ and $u = -1$ in eq. (A1):

$$w_{k,\text{max}} = 1 + [2(1 - \Delta)]^{1/2}. \quad (\text{A3})$$

If $w_k > w_{k,\max}$, the system is guaranteed to be disrupted. For a given $w_{k,\min} < w_k < w_{k,\max}$ and $\Delta < 1/2$, u must be less than a maximum value, u_{\max} , for the binary to remain bound following the explosion:

$$u < u_{\max} \equiv \frac{1}{2w_k}(1 - 2\Delta - w_k^2) . \quad (\text{A4})$$

When the kick speed is large ($w_k \gtrsim 1$), we see that $u_{\max} < 0$. Therefore, if the directions of the kicks are preferentially aligned perpendicularly to the orbital plane (i.e., $u \sim 0$), rather than distributed isotropically, we expect somewhat fewer bound and retained systems for a mean kick speed that is larger than the typical orbital speed (see Brandt & Podsiadlowski 1995). Conversely, if the mean kick speed is small, perpendicular kicks tend to yield an increase in the number of retained binaries, although the baseline retention fraction (for isotropic kicks) is also larger in this case.

The center-of-mass (CM) speed of a bound binary determines whether or not the system will be retained in the cluster. The CM speed, w_{CM} , following the explosion is given by

$$w_{\text{CM}} = \frac{1}{1+q'}[(q'\Delta)^2 - 2q'\Delta u w_k + w_k^2]^{1/2} . \quad (\text{A5})$$

If w_{esc} is the dimensionless central escape speed of the cluster, then the probability that a bound post-SN binary is retained is simply a step function, $S(w_{\text{esc}} - w_{\text{CM}})$, equal to unity for $w_{\text{esc}} - w_{\text{CM}} > 0$ and vanishing otherwise. Taking Δ , q' , and w_{esc} to be fixed parameters, we obtain the retention probability, P_r , as a function of w_k by integrating over u :

$$P_r(w_k; \Delta, q', w_{\text{esc}}) = \int_{-1}^{\min(1, u_{\max})} du p(u) S(w_{\text{esc}} - w_{\text{CM}}) , \quad (\text{A6})$$

where $\min(1, u_{\max})$ is the minimum of 1 and u_{\max} . For isotropically distributed kick directions, the distribution function for u is simply $p(u) = 1/2$. Convolution of P_r with the distribution in dimensionless kick speeds, $p(w_k)$, yields the total probability, $P_{r,\text{tot}}$, that a bound binary is retained in the cluster after the SN:

$$P_{r,\text{tot}}(\Delta, q', w_{\text{esc}}) = \int_0^{w_{k,\max}} dw_k p(w_k) P_r(w_k; \Delta, q', w_{\text{esc}}) \quad (\text{A7})$$

B. SUPERNOVAE IN ECCENTRIC BINARIES

In this Appendix, we present a flexible, computationally convenient formulation of the equations that describe a binary system following an asymmetric SN (SN) explosion of one of the components. We allow for the possibility that the pre-SN binary is eccentric, and we consider the effects of instantaneous mass loss from the exploding star and an impulsive kick delivered to the newly-formed compact remnant. Also included in our analysis is the effect of the SN blast wave on the companion to the exploding star. Furthermore, if the binary is disrupted following the SN, we calculate the asymptotic velocities of the components. Our approach differs from previous studies (e.g., Hills 1983; Brandt & Podsiadlowski 1995; Tauris & Takens 1998) in that we use mathematically compact vector expressions to describe the binary system after the explosion. It is straightforward to directly implement this vector formalism in a computer code, since vector arithmetic can be performed using simple array operations.

Consider a pre-SN binary system that consists of stars with masses M_1 and M_2 in an orbit with semimajor axis a and eccentricity e . The Keplerian orbital frequency is given by $\Omega = (GM_b/a^3)^{1/2}$, where $M_b = M_1 + M_2$. Relative to the center-of-mass (CM), the positions of the two stars at some time t are $\mathbf{r}_1(t)$ and $\mathbf{r}_2(t)$, and the corresponding velocities are $\mathbf{v}_1(t)$ and $\mathbf{v}_2(t)$. The relative positions and velocities are given by $\mathbf{r}(t) = \mathbf{r}_1(t) - \mathbf{r}_2(t)$ and $\mathbf{v}(t) = \mathbf{v}_1(t) - \mathbf{v}_2(t)$, respectively.

It is convenient to have a coordinate-independent description of the binary system. Such a description is provided by the two conserved vectors of the Kepler problem, namely the angular momentum per unit reduced mass, \mathbf{h} , and the Laplace-Runge-Lenz (LRL) vector, \mathbf{e} (e.g., Goldstein 1980; Eggleton 1999):

$$\mathbf{h} = \mathbf{r} \times \mathbf{v} \quad ; \quad \mathbf{e} = \frac{\mathbf{v} \times \mathbf{h}}{GM_b} - \frac{\mathbf{r}}{r} . \quad (\text{B1})$$

Note that \mathbf{h} points perpendicular to the orbital plane and has a magnitude $h = \Omega a^2(1-e^2)^{1/2}$, and \mathbf{e} points in the direction of periastron of star 1 and has a magnitude equal to the orbital eccentricity, e . By convention, boldfaced characters denote vectors, while the same characters with normal typeface denote the magnitudes of those vectors.

Since we allow for the possibility that the pre-SN binary is eccentric, we must take some care in computing \mathbf{r} and \mathbf{v} at the time of the explosion. We assume that there is no preferred position along the orbit for the explosion to take place; therefore, the explosion probability per unit time is constant. No closed form expressions exist for \mathbf{r} and \mathbf{v} as functions of time, and so we must be content with a parametric representation. Consider a Cartesian coordinate system with x -, y -, and z -axes defined by the directions of \mathbf{e} , $\mathbf{h} \times \mathbf{e}$, and \mathbf{h} , respectively. In terms of the eccentric anomaly, E , the dynamical equations read

$$\Omega t_p = E - e \sin E \quad (\text{B2})$$

$$x = a(\cos E - e) \quad ; \quad y = a(1 - e^2)^{1/2} \sin E \quad (\text{B3})$$

$$v_x = -\frac{\Omega a^2}{r} \sin E \quad ; \quad v_y = \frac{\Omega a^2}{r}(1 - e^2)^{1/2} \cos E , \quad (\text{B4})$$

where t_p is the time elapsed since periastron passage. With a randomly selected value for Ωt_p , the corresponding value of E is obtained by solving eq. (B2) numerically, and the relative position and velocity vectors can be readily computed.

At the randomly selected time, star 1 undergoes a SN explosion. We assume that the explosion is an impulsive event, meaning that the direct dynamical influence of the explosion occurs over a time that is much shorter than the orbital period. In other words, it is assumed the SN explosion and the associated blast wave have an instantaneous effect on the masses and velocities of the binary components. The envelope of star 1 is ejected, exposing a remnant of mass M'_1 with a new velocity $\mathbf{v}'_1 = \mathbf{v}_1 + \Delta\mathbf{v}_1$, where $\Delta\mathbf{v}_1$ is the kick velocity. The magnitude and direction of the kick velocity are chosen from appropriate distributions (see § 3). After a negligibly short time (the time it takes the blast wave to cross the orbit), a small fraction of the blast wave will interact with star 2, resulting in a new mass M'_2 and velocity $\mathbf{v}'_2 = \mathbf{v}_2 + \Delta\mathbf{v}_2$, where $\Delta\mathbf{v}_2$ is directed antiparallel to \mathbf{r} (see Wheeler, Lecar, & McKee 1975; Fryxell & Arnett 1981). If star 2 is still on the main sequence at the time of the explosion, it is expected the SN ejecta has only a small effect on star 2 and on the binary orbit. However, if star 2 is a giant at the time of the SN, a large fraction of its envelope may be stripped by the blast wave (see, however, Livne, Tuchman, & Wheeler 1992; Marietta, Burrows, & Fryxell 2000), and so we consider this possibility in our mathematical formalism.

The combined effects of mass loss and the velocity perturbations received by the binary components yield a CM velocity

$$\begin{aligned} \mathbf{v}'_{\text{CM}} &= \frac{1}{M'_b} [M'_1 \mathbf{v}'_1 + M'_2 \mathbf{v}'_2] \\ &= \left(-\frac{M_2}{M'_b} \frac{\Delta M_1}{M_b} + \frac{M_1}{M'_b} \frac{\Delta M_2}{M_b} \right) \mathbf{v} + \frac{M'_1}{M'_b} \Delta\mathbf{v}_1 + \frac{M'_2}{M'_b} \Delta\mathbf{v}_2, \end{aligned} \quad (\text{B5})$$

where $\Delta M_1 = M_1 - M'_1$ is the mass of the ejected envelope of star 1, $\Delta M_2 = M_2 - M'_2$ is the mass stripped and ablated from star 2 (Wheeler, Lecar, & McKee 1975), and $M'_b = M'_1 + M'_2$. The orbital parameters following the explosion may differ dramatically from their initial values. In fact, the explosion may disrupt the binary entirely. The post-SN orbital parameters are determined by the new specific angular momentum, \mathbf{h}' , and the new LRL vector, \mathbf{e}' :

$$\mathbf{h}' = \mathbf{r} \times \mathbf{v}' \quad ; \quad \mathbf{e}' = \frac{\mathbf{v}' \times \mathbf{h}'}{GM'_b} - \frac{\mathbf{r}}{r}. \quad (\text{B6})$$

The binary is gravitationally bound following the SN if $e' < 1$. In this case, the post-SN semimajor axis is given by

$$a' = \frac{h'^2}{GM'_b(1 - e'^2)}. \quad (\text{B7})$$

It is sometimes interesting to know the spin-orbit misalignment angle, γ , of the compact remnant or its companion following the SN (e.g., Brandt & Podsiadlowski 1995; Kalogera 2000). Star 2 will have the same rotation sense as the orbit following a phase of mass accretion. In this case, the spin of star 2 preserves the direction of the pre-SN orbital angular momentum, and the cosine of the misalignment angle is simply

$$\cos \gamma = \hat{\mathbf{h}} \cdot \hat{\mathbf{h}}', \quad (\text{B8})$$

where hats denote unit vectors. Star 1 may likewise spin in the direction of the orbit owing to tidal coupling; however, this is not necessarily true for the remnant (see Spruit & Phinney 1998).

On the other hand, if $e' > 1$, the compact remnant and star 2 are not gravitationally bound, and we would like to compute the asymptotic speeds of the components relative to the pre-SN CM velocity. In the new CM frame, the two objects recede along hyperbolic trajectories. As a function of the true anomaly (also the polar angle in the new orbital plane), θ , the relative separation increases according to $r(\theta) \propto (1 + e' \cos \theta)^{-1}$. Clearly, r approaches infinity as $\cos \theta$ approaches the value $-1/e'$. For large r , the direction of the relative velocity is nearly radial, and so the relative velocity at infinity, \mathbf{v}_∞ , is given by

$$\mathbf{v}_\infty = v_\infty \left[-\frac{1}{e'} \hat{\mathbf{e}}' + \left(1 - \frac{1}{e'^2} \right)^{1/2} \hat{\mathbf{h}}' \times \hat{\mathbf{e}}' \right], \quad (\text{B9})$$

where

$$v_\infty = \frac{GM'_b}{h'} (e'^2 - 1)^{1/2}. \quad (\text{B10})$$

Given \mathbf{v}_∞ and \mathbf{v}'_{CM} , the asymptotic velocities of the components relative to the pre-SN CM velocity can be computed:

$$\mathbf{v}_{1,\infty} = \frac{M'_2}{M'_b} \mathbf{v}_\infty + \mathbf{v}'_{\text{CM}} \quad ; \quad \mathbf{v}_{2,\infty} = -\frac{M'_1}{M'_b} \mathbf{v}_\infty + \mathbf{v}'_{\text{CM}}. \quad (\text{B11})$$

REFERENCES

- Abt, H. A. & Levy, S. G. 1978, *ApJS*, 36, 241
- Anderson, S. B. 1993, Ph. D. thesis, Caltech
- Anderson, S. B., Wolszczan, R., Kulkarni, S. R., & Prince, T. A. 1997, *ApJ*, 482, 870
- Arras, P., & Lai, D. 1999, *ApJ*, 519, 745
- Bacon, D., Sigurdsson, S., & Davies, M. B. 1996, *MNRAS*, 281, 830
- Bailyn, C. D., & Grindlay, J. E. 1990, *ApJ*, 353, 159
- Biehle, G. T. 1991, *ApJ*, 380, 167
- Biggs, J. D., Bailes, M., Lyne, A. G., Goss, W. M., & Fruchter, A. S. 1994, *MNRAS*, 267, 125
- Bildsten, L., et al. 1997, *ApJS*, 113, 367
- Binney, J., & Tremaine, S. 1987, Princeton, NJ, Princeton University Press, 1987, p. 42
- Blaauw, A. 1961, *Bull. Astron. Inst. Netherlands*, 15, 265
- Boersma, J. 1961, *Bull. Astron. Inst. Netherlands*, 15, 291
- Bonnell, I. A., Bate, M. R., & Zinnecker, H. 1998, *MNRAS*, 298, 93
- Brandt, N., & Podsiadlowski, Ph. 1995, *MNRAS*, 274, 461
- Braun, H., & Langer, N. 1995, *A&A*, 297, 483
- Brown, G. E., Lee, C.-H., & Bethe, H. A. 2000, *ApJ*, 541, 918
- Camilo, F., Lorimer, D. R., Freire, P., Lyne, A. G., & Manchester, R. N. 2000, *ApJ*, 535, 975
- Cannon, R. C. 1993, *MNRAS*, 263, 817
- Caraveo, P. A. 1993, *ApJ*, 415, L111
- Chen, K., & Leonard, P. J. T. 1993, *ApJ*, 411, L75
- Chevalier, R. A. 1993, *ApJ*, 411, L33
- Chevalier, R. A. 1996, *ApJ*, 459, 322
- Chernoff, D. F., & Weinberg, M. D. 1990, *ApJ*, 351, 121
- Cordes, J. M. 1986, *ApJ*, 311, 183
- Cordes, J. M., & Chernoff, D. F. 1998, *ApJ*, 505, 315
- Cowley, A. P. 1969, *PASP*, 81, 297
- Cowley, A. P., Hutchings, J. B., & Popper, D. M. 1977, *PASP*, 89, 882
- D'Amico, N., Possenti, A., Manchester, R. N., Sarkissian, J., Lyne, A. G., & Camilo, F. 2001, Abstracts of the 20th Texas Symposium on Relativistic Astrophysics, held in Austin, Texas, Dec. 10-15, 2000, astro-ph/0105122
- Darwin, G. H. 1879, *Phil. Trans. Roy. Soc.*, 170, 1
- Davies, M. B. 1995, *MNRAS*, 276, 887
- Davies, M. B., & Hansen, B. M. S. 1998, *MNRAS*, 301, 15
- De Greve, J.-P., & de Loore, C. 1977, *Ap&SS*, 50, 75
- Delgado, A. J. & Thomas, H. -. 1981, *A&A*, 96, 142
- Delgado-Martí, H., Levine, A. M., Pfahl, E., & Rappaport, S. A. 2001, *ApJ*, 546, 455
- Deutsch, E. W., Margon, B., & Anderson, S. F. 2000, *ApJ*, 530, L21
- Dewey, R. J., & Cordes, J. M. 1987, *ApJ*, 321, 780
- Dewi, J. D. M., & Tauris, T. M. 2000, *A&A*, 360, 1043
- Di Stefano, R., & Rappaport, S. 1992, *ApJ*, 396, 587
- Drukier, G. A. 1996, *MNRAS*, 280, 498
- Duquennoy, A., & Mayor, M. 1991, *A&A*, 248, 485
- Eggleton, P. P. 1983, *ApJ*, 268, 368
- Eggleton, P. P., Fitchett, M. J., & Tout, C. A. 1989, *ApJ*, 347, 998
- Eggleton, P. 1999, *Evolutionary Processes in Binary and Multiple Stars* (Cambridge: Cambridge Univ. Press), in preparation
- Elmegreen, B. G. 2000, *ApJ*, 530, 277
- Fabian, A. C., Pringle, J. E., & Rees, M. J. 1975, *MNRAS*, 172, 15P
- Flannery, B. P., & van den Heuvel, E. P. J. 1975, *A&A*, 39, 61
- Frail, D. A., Goss, W. M., & Whiteoak, J. B. Z. 1994, *ApJ*, 437, 781
- Freire, P. C., Camilo, F., Lorimer, D. R., Lyne, A. G., & Manchester, R. N. 2000, *ASP Conf. Ser.* 202: IAU Colloq. 177: Pulsar Astronomy - 2000 and Beyond, 87
- Fruchter, A. S., & Goss, W. M. 2000, *ApJ*, 536, 865
- Fryer, C. L., Benz, W., & Herant, M. 1996, *ApJ*, 460, 801
- Fryer, C., & Kalogera, V. 1997, *ApJ*, 489, 244
- Fryer, C., Burrows, A., & Benz, W. 1998, *ApJ*, 496, 333
- Fryer, C. L., & Heger, A. 2000, *ApJ*, 541, 1033
- Fryxell, B. A., & Arnett, W. D. 1981, *ApJ*, 243, 994
- Fukuda, I. 1982, *PASP*, 94, 271
- Gaensler, B. M., & Frail, D. A. 2000, *Nature*, 406, 158
- Garmany, C. D., Conti, P. S., & Massey, P. 1980, *ApJ*, 242, 1063
- Goldstein, H. 1980, *Classical Mechanics*, (Reading, MA: Addison-Wesley), 102
- Grindlay, J. E. 1987, *IAU Symp.* 125: The Origin and Evolution of Neutron Stars, 125, 173
- Grindlay, J. E., Heinke, C., Edmonds, P. D., & Murray, S. S. 2001, *Science*, in press
- Gunn, J. E., & Ostriker, J. P. 1970, *ApJ*, 160, 979
- Habets, G. M. H. J. 1986a, *A&A*, 165, 95
- Habets, G. M. H. J. 1986b, *A&A*, 167, 61
- Hachisu, I., Kato, M., & Nomoto, K. 1999, *ApJ*, 522, 487
- Han, Z. 1998, *MNRAS*, 296, 1019
- Hansen, B. M. S., & Phinney, E. S. 1997, *MNRAS*, 291, 569
- Harmanec, P. et al. 2000, *A&A*, 364, L85
- Harris, W. E. 1996, *AJ*, 112, 1487
- Harrison, E. R., & Tademaru, E. 1975, *ApJ*, 201, 447
- Heger, A., Langer, N., & Woosley, S. E. 2000, *ApJ*, 528, 368
- Helfand, D. J., & Tademaru, E. 1977, *ApJ*, 216, 842
- Hewish, A., Bell, S. J., Pilkington, J. D., Scott, P. F., & Collins, R. A. 1968, *Nature*, 217, 709
- Hills, J. G. 1976, *MNRAS*, 175, 1P
- Hills, J. G. 1983, *ApJ*, 267, 322
- Hjellming, M. S., & Webbink, R. F. 1987, *ApJ*, 318, 794
- Hoogerwerf, R., de Bruijne, J. H. J., & de Zeeuw, P. T. 2001, *A&A*, 365, 49
- Hurley, J. R., Pols, O. R., & Tout, C. A. 2000, *MNRAS*, 315, 543
- Hut, P. 1981, *A&A*, 99, 126
- Hut, P., Murphy, B. W., & Verbunt, F. 1991, *A&A*, 241, 137
- Iben, I. 1982, *ApJ*, 259, 244
- Iben, I., & Tutukov, A. V. 1984, *ApJS*, 54, 335
- Iben, I. J., & Tutukov, A. V. 1996, *ApJ*, 456, 738
- in 't Zand, J. J. M., Corbet, R. H. D., & Marshall, F. E. 2001, *ApJ*, 553, L165
- Johnston, H. M., & Verbunt, F. 1996, *A&A*, 312, 80
- Joshi, K. J., Nave, C. P., & Rasio, F. A. 2001, *ApJ*, 550, 691
- Kähler, H. 1989, *A&A*, 209, 67
- Kalogera, V., & Webbink, R. F. 1998, *ApJ*, 493, 351
- Kalogera, V. 2000, *ApJ*, 541, 319
- Kaspi, V. M., Bailes, M., Manchester, R. N., Stappers, B. W., & Bell, J. F. 1996, *Nature*, 381, 584
- Katz, J. I. 1983, *A&A*, 128, L1
- Kelley, R. L., Rappaport, S., & Ayasli, S. 1983, *ApJ*, 274, 765
- Kippenhahn, R., & Weigert, A. 1966, *Zeitschrift Astrophysics*, 65, 251
- Kraicheva, Z. T., Popova, E. I., Tutukov, A. V., & Yungelson, L. R. 1978, *Soviet Astronomy*, 22, 670
- Kroupa, P., Tout, C. A., & Gilmore, G. 1993, *MNRAS*, 262, 545
- Lai, D. 2000, in *Physics of Neutron Star Interiors*, ed. Blaschke, D., Glendenning, N. K., & Sedrakian, A. (Springer), astro-ph/0012049
- Lai, D., Chernoff, D. F., & Cordes, J. M. 2001, *ApJ*, 549, 1111
- Langer, N. 1989, *A&A*, 220, 135
- Langer, N., & Maeder, A. 1995, *A&A*, 295, 685
- Lauterborn, D. 1970, *A&A*, 7, 150
- Leonard, P. J. T., Hills, J. G., & Dewey, R. J. 1994, *ApJ*, 423, L19
- Lewin, W. H. G., van Paradijs, J., & Taam, R. E. 1993, *Space Science Reviews*, 62, 223
- Livne, E., Tuchman, Y., & Wheeler, J. C. 1992, *ApJ*, 399, 665
- Lorimer, D. R., Bailes, M., & Harrison, P. A. 1997, *MNRAS*, 289, 592
- Lyne, A. G., Anderson, B., & Salter, M. J. 1982, *MNRAS*, 201, 503
- Lyne, A. G., & Lorimer, D. R. 1994, *Nature*, 369, 127
- Lyne, A. G., Manchester, R. N., & D'Amico, N. 1996, *ApJ*, 460, L41
- Lyne, A. G., Mankelow, S. H., Bell, J. F., & Manchester, R. N. 2000, *MNRAS*, 316, 491
- Maeder, A. 1992, *A&A*, 264, 105
- Marietta, E., Burrows, A., & Fryxell, B. 2000, *ApJS*, 128, 615
- Marigo, P., Girardi, L., Chiosi, C., & Wood, P. R. 2001, *A&A*, 371, 152
- Mason, B. D., Gies, D. R., Hartkopf, W. I., Bagnuolo, W. G., Brummelaar, T. T., & McAlister, H. A. 1998, *AJ*, 115, 821
- Meyer, F., & Meyer-Hofmeister, E. 1979, *A&A*, 78, 167
- Meylan, G., Sarajedini, A., Jablonka, P., Djorgovski, S. G., Bridges, T., & Rich, R. M. 2001, *AJ*, in press, astro-ph/0105013
- Miller, G. E., & Scalo, J. M. 1979, *ApJS*, 41, 513
- Nelemans, G., Yungelson, L. R., Portegies Zwart, S. F., & Verbunt, F. 2001, *A&A*, 365, 491
- Nelson, C. A., & Eggleton, P. P. 2001, *ApJ*, 552, 664
- Nomoto, K. 1982, *ApJ*, 253, 798
- Nomoto, K., & Iben, I. 1985, *ApJ*, 297, 531
- Nomoto, K. 1987, *IAU Symp.* 125: The Origin and Evolution of Neutron Stars, 125, 281
- Nomoto, K., & Kondo, Y. 1991, *ApJ*, 367, L19
- Paczynski, B., & Sienkiewicz R. 1972, *Acta Astron.*, 22, 73
- Paczynski, B. 1990, *ApJ*, 348, 485
- Pfahl, E., & Rappaport 2001, *ApJ*, in press
- Podsiadlowski, Ph., Joss, P. C., & Hsu, J. J. L. 1992, *ApJ*, 391, 246
- Podsiadlowski, Ph., Hsu, J. J. L., Joss, P. C., & Ross, R. R. 1994, in *Circumstellar Media in the Late Stages of Stellar Evolution*, ed. Clegg, R. E. S., Stevens, I. R., & Meikle, W. P. S. (Cambridge University Press: Cambridge), 187
- Podsiadlowski, Ph., Cannon, R. C., & Rees, M. J. 1995, *MNRAS*, 274, 485
- Podsiadlowski, Ph., Rappaport, S., & Pfahl, E. 2001, *ApJ*, submitted
- Pols, O. R. 1994, *A&A*, 290, 119
- Preibisch, T., Hofmann, K. -, Schertl, D., Weigelt, G., Balega, Y., Balega, I., & Zinnecker, H. 2000, *IAU Symposium*, 200, 106P

- Prialnik, D. & Kovetz, A. 1995, *ApJ*, 445, 789
- Price, N. M., & Podsiadlowski, Ph. 1995, *MNRAS*, 273, 1041
- Rappaport, S., Joss, P. C., & Webbink, R. F. 1982, *ApJ*, 254, 616
- Rappaport, S., Di Stefano, R., & Smith, J. D. 1994, *ApJ*, 426, 692
- Rappaport, S., Pfahl, E., Rasio, F., & Podsiadlowski, Ph. 2000, in *Evolution of Binary and Multiple Star Systems*, ed. Podsiadlowski, Ph., Rappaport, S., King, A. R., D'Antona, F., & Burderi, L. (Sheridan: Chelsea), 409, astro-ph/0101535
- Rasio, F. A., & Shapiro, S. L. 1991, *ApJ*, 377, 559
- Rasio, F. A., & Shapiro, S. L. 1995, *ApJ*, 438, 887
- Rasio, F. A., Pfahl, E. D., & Rappaport, S. 2000, *ApJ*, 532, L47
- Saffer, R. A., Livio, M., & Yungelson, L. R. 1998, *ApJ*, 502, 394
- Salpeter, E. E. 1955, *ApJ*, 121, 161
- Sandquist, E. L., Taam, R. E., & Burkert, A. 2000, *ApJ*, 533, 984
- Scalo, J. M. 1986, *Fundamentals of Cosmic Physics*, 11, 1
- Shklovskii, I. S. 1970, *Soviet Astronomy*, 13, 562
- Sigurdsson, S., & Phinney, E. S. 1993, *ApJ*, 415, 631
- Sigurdsson, S. & Phinney, E. S. 1995, *ApJS*, 99, 609
- Spruit, H. C., & Phinney, E. S. 1998, *Nature*, 393, 139
- Spruit, H. C. 1998, *A&A*, 333, 603
- Taam, R. E., Bodenheimer, P., & Ostriker, J. P. 1978, *ApJ*, 222, 269
- Takahashi, K., & Portegies Zwart, S. F. 2000, *ApJ*, 535, 759
- Tauris, T. M., & Takens, R. J. 1998, *A&A*, 330, 1047
- Taylor, J. H., & Cordes, J. M. 1993, *ApJ*, 411, 674
- Terman, J. L., Taam, R. E., & Savage, C. O. 1998, *MNRAS*, 293, 113
- Thorne, K. S., & Zytlow, A. N. 1975, *ApJ*, 199, L19
- Thorne, K. S., & Zytlow, A. N. 1977, *ApJ*, 212, 832
- van den Heuvel, E. P. J., Bhattacharya, D., Nomoto, K., & Rappaport, S. A. 1992, *A&A*, 262, 97
- van den Heuvel, E. P. J., & van Paradijs, J. 1997, *ApJ*, 483, 399
- Verbunt, F., & van den Heuvel, E. P. J. 1995, in *X-ray Binaries*, ed. Lewin, W. H. G., van Paradijs, J., & van den Heuvel, E. P. J. (Cambridge University Press: Cambridge), 457
- Verbunt, F., & Hasinger, G. 1998, *A&A*, 336, 895
- Verbunt, F. 2001, *A&A*, 368, 137
- Webbink, R. F. 1984, *ApJ*, 277, 355
- Wellstein, S. & Langer, N. 1999, *A&A*, 350, 148
- Wellstein, S., Langer, N., & Braun, H. 2001, *A&A*, 369, 939
- Wheeler, J. C., Lecar, M., & McKee, C. F. 1975, *ApJ*, 200, 145
- Wilson, C. A., et al. 1997, *ApJ*, 479, 388